

Figure 4. A stereodiagram of the molecule based on experimentally determined heavy atom positions and assumed hydrogen atom positions.

Packing of the molecules in the unit cell is shown in Figure 2. Dotted lines indicate the closest approaches between molecules. The smallest intermolecular distances are 3.4 Å between C=O...Me and 3.8 Å between Me...Me, normal van der Waals separations.

**Acknowledgment.** We wish to thank Dr. Bernhard Witkop of the National Institutes of Health for introducing us to the problem and Dr. Jerome Karle of the Naval Research Laboratory for his continuing interest and helpful suggestions.

## A Spectroscopic Study of the Polarized Luminescence of Indoles<sup>1</sup>

Pill-Soon Song<sup>1</sup> and William E. Kurtin<sup>2</sup>

Contribution from the Department of Chemistry, Texas Technological University, Lubbock, Texas 79409. Received February 24, 1969

**Abstract:** The method of photoselection has been used to determine the polarized fluorescence excitation and emission spectra of indole and several of its derivatives. The results are compared with theoretical predictions from the P-P-P SCF MO-CI method. The first and second ( $\pi, \pi^*$ ) states were assigned as  $^1L_b$  and  $^1L_a$ , respectively, in all cases studied. Emission from both  $^1L_a$  and  $^1L_b$  0-0 states has been confirmed in most of the indoles studied on the basis of sharp changes in the degree of polarization of the fluorescence bands with the possible exception of indole-N-acetic acid. The dual emission seems to occur in both glycerol-methanol (9:1, 263°K) and in an EPA rigid glass (77°K). The polarized phosphorescence spectra and mean lifetimes have also been obtained at 77°K in EPA glass. The triplet-singlet emission in seven indole derivatives has been shown to originate from  $^3(\pi, \pi^*)$  states of  $^3L_a$  type. The 0-0 phosphorescence emission bands were found to be negatively polarized, indicating predominant out-of-plane polarizations. Significant vibronic activity along the phosphorescence bands has been revealed, and in particular the degree of polarization increases considerably beyond the 0-0 bands of the carboxyl and formyl indoles. The possible contributions of various states (out-of-plane  $n, \pi^*$ ,  $\sigma, \pi^*$ , or  $\pi, \sigma^*$ , and in-plane  $\pi, \pi^*$ ) to the triplet-singlet transition probability via (a) direct spin-orbit, (b) spin vibronic (first order), and (c) vibronic spin-orbit (second order) couplings have been discussed qualitatively.

The study of the electronic structure in the excited states of biomolecules has increased markedly in the past decade, primarily because of an increased interest in their photochemical and photobiological reactivities.<sup>3-6</sup> Many biomolecules, because of their complex structure, often present unusually interesting spectroscopic and photochemical problems. Flavins and indoles are two of these types of molecules. We

have previously reported on the nature of the excited singlet and triplet states of flavins using both theoretical and experimental methods.<sup>7-11</sup> Theoretically and spectroscopically, indole and its derivatives are of considerable interest. Platt<sup>12</sup> suggested a spectroscopic correlation based on the positions and intensities of the electronic bands, and placed indole between indene and naphthalene (isoelectronic with indole). Several workers have noted some peculiarities in the indole luminescence. Schutt and Zimmermann<sup>13</sup> observed an unusual dual fluorescence emission from both  $L_a$  and  $L_b$  states of indole. This result has not been re-

(1) To whom reprint requests should be sent.

(2) Part III of the series, "Photochemistry of the Model Phototropic System Involving Flavins and Indoles." Supported by the Robert A. Welch Foundation (Grant No. D-182) and National Science Foundation (Grant No. GB-8055). W. E. K. is a predoctoral fellow of the Robert A. Welch Foundation.

(3) A number of review articles and monographs are available. For examples, see ref 4-6.

(4) W. D. McElroy and B. Glass, Ed., "Light and Life (Symposium Volume)," The Johns Hopkins University Press, Baltimore, Md., 1961.

(5) S. V. Konev, "Fluorescence and Phosphorescence of Proteins and Nucleic Acids," Plenum Press, New York, N. Y., 1967.

(6) H. H. Seliger and W. D. McElroy, "Light: Physical and Biological Action," Academic Press, New York, N. Y., 1965.

(7) W. E. Kurtin and P. S. Song, *Photochem. Photobiol.*, **7**, 263 (1968).

(8) P. S. Song and W. E. Kurtin, *J. Am. Chem. Soc.*, **89**, 4248 (1967).

(9) P. S. Song, *J. Phys. Chem.*, **72**, 536, 4724 (1968).

(10) W. E. Kurtin and P. S. Song, *Photochem. Photobiol.*, **9**, 127 (1969).

(11) P. S. Song, *Intern. J. Quantum Chem.*, in press.

(12) J. R. Platt, *J. Chem. Phys.*, **19**, 101 (1951).

(13) H. U. Schutt and H. Zimmermann, *Z. Elektrochem.*, **67**, 54 (1963).

examined. We will comment on this interesting point later. Another peculiar aspect of the indole luminescence is its large Stokes shift.<sup>14-20</sup>

For the above reasons and also for its biological implications, we undertook an extensive spectroscopic study of indole emission with the aid of luminescence polarizations and molecular orbital calculations. The indole derivatives studied were indole-3-acetic acid, indole-N-acetic acid, indole-2-carboxylic acid, indole-3-carboxylic acid, indole-5-carboxylic acid, and indole-3-aldehyde, along with indole itself. There are additional reasons for studying these particular derivatives. First, indole-3-acetic acid is known to be a constituent of the phototropic apparatus in higher plants,<sup>21</sup> and is decarboxylated in the photoreaction with riboflavin.<sup>22</sup> Various photoproducts, including carboxylic and aldehydic derivatives, are formed by oxidation of the side chain. Therefore, some of the derivatives used in the present study serve as analogs for the phototropic constituent. Secondly, while indole itself has been the subject of the spectroscopic studies of many workers, the emission spectroscopy of indole derivatives, particularly with electron-withdrawing substituents, has not been thoroughly investigated. Thirdly, the effects of the substituent and its position on  $^1L_b$ ,  $^1L_a$ , and the lowest triplet ( $^3L_a$ ) state will be dealt with in this paper. There is also a practical reason, since the indoles chosen are reasonably soluble in both polar and nonpolar solvents.

## Experimental Section

**Materials.** Indole (I) was purissimum grade from the Aldrich Chemical Co. and further purified by recrystallization from an ethanol-water mixture, or by vacuum sublimation using a McCarter vacuum sublimator. Indole-3-acetic acid (II) was the pfs grade (white crystals) obtained from Sigma Chemical Co. and was used without further purification. Indole-N-acetic acid (III), indole-2-carboxylic acid (IV), indole-3-carboxylic acid (V), and indole-5-carboxylic acid (VI) from Aldrich Chemical Co. (research grade) and indole-3-aldehyde (VII, pfs grade white crystals) from Sigma Chemical Co. were purified in the same manner as indole. Ethanol (absolute) was USP grade from the U. S. Industrial Chemical Co. and was distilled four times. Methanol (absolute) was reagent grade obtained from the Baker and Adamson Co., and redistilled. Ethylene glycol was reagent grade from the Baker Co., and used without further purification. Glycerol, diethyl ether, and isopentane, all spectroquality, were obtained from the Matheson Co. A spectroquality EPA mixture (diethyl ether, isopentane, and ethanol; 5:5:2) from American Instrument Co. was also used. Water was deionized and then twice redistilled.

**Fluorescence Polarization Spectra.** The method used here has previously been described in detail.<sup>7</sup> The details of the experiments were essentially the same. The concentrations of the various indoles were kept low (*ca.*  $10^{-5}$  M) in order to avoid concentration depolarization, as observed by Weber.<sup>23</sup> Table I lists the wavelengths used for the polarization measurements.

**Phosphorescence Spectra.** The phosphorescence excitation (source: Hanovia xenon arc lamp) and emission (PM tube: RCA 1P 28) spectra were obtained on the Aminco-Bowman spectrofluorometer using the Aminco-Keirs phosphoroscope attach-

**Table I.** Wavelengths ( $m\mu$ ) Used in Polarization Measurements

Compound	Fluorescence		Phosphorescence	
	Excitation	Emission	Excitation	Emission
Indole	285	345	290	435
Indole-3-acetic acid	285	355	290	440
Indole-N-acetic acid	285	355	290	440
Indole-2-carboxylic acid	305	380	305	500
Indole-3-carboxylic acid	295	345	295	427
Indole-5-carboxylic acid	295	415	290	445
Indole-3-aldehyde	285	345	300	435

ment. The spectra (uncorrected, unless otherwise indicated) were measured at 77°K in EPA glass. The concentrations of the indoles were approximately  $10^{-4}$  M in all cases. Table I also lists the wavelengths employed for these measurements.

**Phosphorescence Lifetimes.** The lifetimes were measured on an X-Y recorder equipped with a time-base scan operation. When the irradiation source is cut off, an exponential decay curve is obtained from which the lifetime is calculated.

**Phosphorescence Polarization Spectra.** The phosphorescence emission and excitation polarization spectra were measured at 77°K in the same manner as the fluorescence polarization spectra.<sup>7</sup> The instrumental depolarization effects have been corrected according to the procedure of Azumi and McGlynn<sup>24</sup> and as described previously.<sup>7</sup> In the measurement of the phosphorescence excitation polarization a minor problem was encountered with the indole molecules, which have relatively long lifetimes (2-6 sec). If the scan speed is too fast, it cannot be assured that the excited triplet state will have decayed sufficiently to ensure steady-state conditions as the excitation wavelength is changed. For this reason, the slowest recorder scan rate attainable in our instrument unit was employed. All spectra reported here have been repeated at least five times to ensure reproducibility.

**Absorption Spectra.** All absorption spectra were recorded on a Bausch and Lomb Spectronic 600 spectrophotometer. The concentrations were the same as those used in the fluorescence polarization experiments.

**Relative Luminescence Yields.** The luminescence spectra (fluorescence and phosphorescence) were recorded using the phosphoroscope attachment by removing the rotating shutter and motor assembly, and then re-covering the bottom of the attachment so as to avoid stray light. The micro dewar containing the sample (all samples having an identical optical density at 265  $m\mu$ ) and liquid nitrogen are then inserted into the sample compartment as is done for recording phosphorescence spectra. Since the shutter is no longer present, the fluorescence in a rigid matrix at 77°K may now also be recorded. After making a correction for the photomultiplier (1P 28) sensitivity using the procedure and data given for an Aminco-Bowman spectrofluorometer by Chen<sup>25</sup> and White, *et al.*,<sup>26</sup> the luminescence intensities were integrated and the ratio of the phosphorescence to fluorescence quantum yield was calculated. The relative luminescence yield (taking indole as unity) was also estimated in the same manner.

**Molecular Orbital Computations.** The well-known Pariser-Parr-Pople (P-P-P) semiempirical SCF MO-CI method in the restricted Hartree-Fock formulation was used to calculate singlet and triplet transition energies, the magnitude and direction of the transition moments, and oscillator strengths. A brief outline of the method as applied to flavins has been given previously,<sup>7</sup> and the details of the various integrals will be described in a forthcoming paper of the present series. The methylene group in the side chains of indole-3-acetic acid and indole-N-acetic acid was treated by the group orbital model.<sup>27</sup> Usually 20-25 singly excited configurations were built into the CI matrix for the excited states of each indole molecule. An all-valence electron calculation based on the SCF MO CNDO/2 approximation developed by Pople, *et al.*,<sup>28</sup> was

- (14) B. L. van Duuren, *J. Org. Chem.*, **26**, 2954 (1961).  
 (15) V. P. Bobrovich, G. S. Kembrovskii, and N. I. Marenko, *Dokl. Akad. Nauk Belorussk. SSR*, **10**, 936 (1966).  
 (16) E. Lippert, *Z. Naturforsch.*, **10a**, 541 (1955).  
 (17) E. Lippert, *Z. Elektrochem.*, **61**, 962 (1957).  
 (18) N. Mataga, Y. Kaifu, and M. Koizumi, *Bull. Chem. Soc. Japan*, **28**, 690 (1955).  
 (19) N. Mataga, Y. Kaifu, and M. Koizumi, *ibid.*, **29**, 465 (1956).  
 (20) J. Eisinger in "Molecular Luminescence (Symposium Volume)," E. C. Lim, Ed., W. A. Benjamin, New York, N. Y., 1969, pp 185-200.  
 (21) See ref 4, pp 646-672.  
 (22) A. W. Galston, *Proc. Natl. Acad. Sci. U. S. A.*, **35**, 10 (1949).  
 (23) G. Weber, ref 4, pp 82-107.

- (24) T. Azumi and S. P. McGlynn, *J. Chem. Phys.*, **37**, 2413 (1962).  
 (25) R. F. Chen, *Anal. Biochem.*, **20**, 339 (1967).  
 (26) C. E. White, M. Ho, and E. Q. Weimer, *Anal. Chem.*, **32**, 438 (1960).  
 (27) R. S. Mulliken, C. A. Rieke, and W. G. Brown, *J. Am. Chem. Soc.*, **63**, 41 (1941).  
 (28) (a) J. A. Pople, D. P. Santry, and G. S. Segal, *J. Chem. Phys.*, **43**, S129, S136 (1965); (b) J. A. Pople and G. A. Segal, *ibid.*, **44**, 3289 (1966).

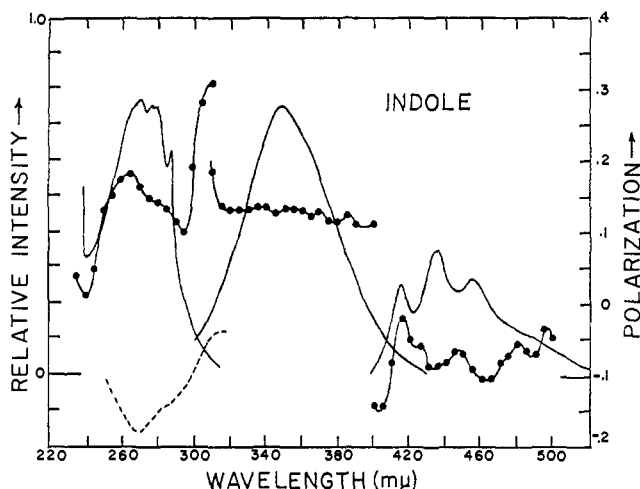


Figure 1. (—): from left to right, the absorption ( $10^{-4} M$  in methanol,  $298^\circ K$ ), fluorescence ( $10^{-4} M$  in methanol,  $298^\circ K$ ), and phosphorescence ( $10^{-4} M$  in EPA,  $77^\circ K$ ) spectra of indole. (—●—●—): from left to right, the polarized fluorescence excitation ( $10^{-5} M$  in glycerol-methanol, 9:1,  $263^\circ K$ ), polarized fluorescence emission ( $10^{-5} M$  in glycerol-methanol, 9:1,  $263^\circ K$ ), and the polarized phosphorescence emission ( $10^{-4} M$  in EPA,  $77^\circ K$ ) spectra of indole. (----): the polarized phosphorescence excitation spectrum ( $10^{-4} M$  in EPA,  $77^\circ K$ ) of indole.

also performed for each indole molecule, and only the pertinent results will be extracted and used in the present work.

## Results

**1. Luminescence Spectra and Electronic Relaxations of Indoles.** Figure 1 shows a summary of the results from various spectral measurements on indole. The absorption spectrum in methanol was obtained at  $298^\circ K$ . The absorption spectrum of indole has been described extensively,<sup>5</sup> and is known to be moderately sensitive to solvent perturbations. However, the room temperature absorption and low temperature ( $77^\circ K$ ) luminescence excitation spectra were essentially identical, as far as the locations of the major electronic bands are concerned. Therefore, both the absorption spectrum at room temperature and the phosphorescence excitation spectrum at  $77^\circ K$  can be used in a mutually complementary manner. The fluorescence spectrum of indole, however, is extremely sensitive to temperature.<sup>20</sup> The fluorescence emission and polarization spectra in Figure 1 were obtained at  $263^\circ K$ , and they are not significantly different from those at  $298^\circ K$ . This is because of the fact that a strong Stokes shift occurs at temperatures between  $170$  and  $230^\circ K$  where the glass softens.<sup>20</sup> The fluorescence polarization spectrum of indole in Figure 1 is very similar to ones obtained previously under slightly different conditions.<sup>23,29</sup> The fluorescence emission spectrum in Figure 1 was obtained by monitoring the emission with an excitation wavelength of  $285 m\mu$ , which roughly corresponds to the long-wavelength  $L_b$  band.<sup>30</sup> However, the  $L_b$  band in this region actually overlaps considerably with the  $L_a$  band,<sup>31</sup> thus making it difficult to assign a particular electronic transition to this particular region of the absorption spectrum. Nevertheless, valuable infor-

(29) G. Weber, *Biochem. J.*, **75**, 335, 345 (1960).

(30) E. A. Chernitskii and S. V. Konev, *Zh. Prikl. Spekt.*, **2**, 261 (1965).

(31) E. A. Chernitskii, S. V. Konev, and V. P. Bobrovich, *Dokl. Akad. Nauk Belorussk. SSR*, **7**, 628 (1963).

mation can be extracted from the low-resolution spectrum. First, the 0-0 fluorescence emission band ( $310 m\mu$  region) appears to have a degree of polarization about the same as the  $265 m\mu$  excitation band which can be assigned to the  ${}^1L_a$  species. But it should be recalled that the fluorescence polarization spectrum was obtained using  $285 m\mu$  excitation, and not the  $265 m\mu$  band (Table I). The  ${}^1L_a$  assignment for the  $265 m\mu$  band will be analyzed in the Discussion section. It is also to be noted that the fluorescence emission polarization smoothly decreases as the frequency decreases along the emission spectrum. In addition, the fluorescence emission lacks vibrational structure. We therefore confirm for the moment the widely accepted assignment that the fluorescence emission from indole in polar solvents is predominantly from the  ${}^1L_a$  state. The gradual decrease in the fluorescence polarization beyond the 0-0 emission band may reflect vibronic activities due to coupling of the  ${}^1L_a$  and  ${}^1L_b$  states, which are closely spaced. The steep increase in the  $305$ – $310 m\mu$  region of the fluorescence excitation polarization can readily be assigned to the 0-0 absorption end of the  ${}^1L_a$  band, while the minimum at  $293 m\mu$  is assigned to the 0-0 absorption end of the  ${}^1L_b$  band. Further details and theoretical results will be discussed later. The polarization in the  $200$ – $235 m\mu$  range has not been recorded due to the inadequacy of the Glan-Thompson excitation polarizer in this region. At this point, we shall defer until later the discussion as to whether the dual emission from  ${}^1L_a$  ( $33,500 cm^{-1}$ ) and  ${}^1L_b$  ( $34,500 cm^{-1}$ ), which is favorable in nonpolar solvents,<sup>13,15,32</sup> is also significant in polar solvents.

The polarized phosphorescence emission spectrum of indole is also shown in Figure 1, along with its excitation polarization and phosphorescence emission spectra. The most apparent fact is that the entire phosphorescence emission band is negatively polarized with respect to the  $290 m\mu$  excitation oscillator. Although the phosphorescence excitation polarization spectrum is not sufficiently accurate due to the experimental difficulty noted in the Experimental Section, it is also clear that both  ${}^1L_a$  and  ${}^1L_b$  transition moments are negatively polarized with respect to the phosphorescence emission oscillator ( $435 m\mu$ ). The 0-0 phosphorescence emission is located at  $404 m\mu$  ( $24,750 cm^{-1}$ ), in good agreement with the 0-0 band at  $405 m\mu$  ( $24,700 cm^{-1}$ ) assigned by Ermolaev<sup>33</sup> and at  $405 m\mu$  ( $24,697 cm^{-1}$ ) assigned by Konev, *et al.*<sup>34</sup> It is obvious that the intensity of the vibronic bands is considerably higher than the 0-0 emission band. Theoretical calculations indicate that the lowest triplet state of aromatic hydrocarbons must be  ${}^3L_a$ .<sup>35</sup> Similarly, we assign the phosphorescence band of indole to the emission from  ${}^3L_a$ . Our MO calculations of indoles support this assignment also, as will be discussed later. The assignment of the lowest triplet as  $L_a$  is experimentally well established for a number of aromatic molecules such as phenanthrene<sup>24</sup> and naphthalene.<sup>36,37</sup>

(32) A. Wieckowski and D. Mechandzjew, *Poznan. Tow. Przyciol. Nauk Pol.*, **11**, 699 (1966).

(33) V. L. Ermolaev, *Opt. Spectry.*, **11**, 266 (1961).

(34) G. S. Kembrovskii, V. P. Bobrovich, and S. V. Konev, *Zh. Prikl. Spektrosk.*, **5**, 695 (1966).

(35) R. Pariser, *J. Chem. Phys.*, **24**, 250 (1956).

(36) H.-J. Czékalla, W. Liptay, and E. Dollfeld, *Ber. Bunsenges. Phys. Chem.*, **68**, 80 (1964).

(37) R. M. Hochstrasser and S. K. Lower, *J. Chem. Phys.*, **40**, 1041 (1964).

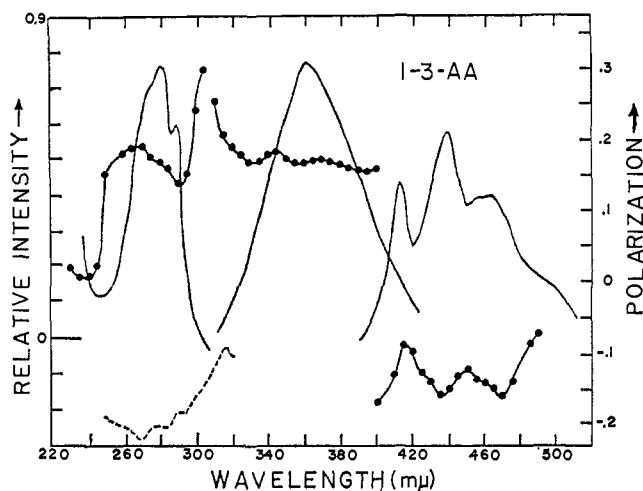


Figure 2. The absorption, emission, and polarization spectra of indole-3-acetic acid. See Figure 1 for legends.

There appear to be two different modes of vibrations in the phosphorescence band structure of indole: vibrations with maximum polarization (*ca.*  $650\text{-cm}^{-1} \pm 100\text{-cm}^{-1}$  series) and those with less polarization (minima in the polarization spectrum, *ca.*  $1500\text{-}1600\text{-cm}^{-1}$  series). Thus, even from the low-resolution phosphorescence polarization spectrum in Figure 1, the following vibrational series can be located:  $415\text{ m}\mu$  ( $24,100\text{ cm}^{-1}$ ;  $1 \times 650\text{ cm}^{-1}$  band),  $426\text{ m}\mu$  ( $23,450\text{ cm}^{-1}$ ;  $2 \times 650\text{ cm}^{-1}$  band),  $446\text{ m}\mu$  ( $22,400\text{ cm}^{-1}$ ;  $3 \times 650\text{ cm}^{-1}$  band),  $482\text{ m}\mu$  ( $20,750\text{ cm}^{-1}$ ;  $5 \times 650\text{ cm}^{-1}$  band), and  $496\text{ m}\mu$  ( $20,160\text{ cm}^{-1}$ ;  $6 \times 650\text{ cm}^{-1}$  band);  $432\text{ m}\mu$  ( $23,150\text{ cm}^{-1}$ ;  $1 \times 1600\text{ cm}^{-1}$  band) and  $462\text{ m}\mu$  ( $21,650\text{ cm}^{-1}$ ;  $2 \times 1600\text{ cm}^{-1}$  band). These band structures in the phosphorescence polarization spectrum of indole were readily reproducible.

Table II lists the relative quantum yields of phosphorescence over fluorescence and the apparent lifetimes of the phosphorescence. The phosphorescence lifetime of  $6.0\text{ sec}$  for indole is similar to that ( $6.3 \pm 0.02\text{ sec}$ ) reported by Ermolaev.<sup>33</sup> The value of Ermolaev was obtained from the phosphorescence decay in an ethyl ether-alcohol glass, instead of an EPA glass as in our case. The difference in matrices may account for our slightly higher value of the ratio of the phosphorescence and fluorescence yields of indole ( $0.32 \pm 0.03$  by Ermolaev). However, as mentioned in the Experimental Section, the relative yields reported in Table II are only "qualitative," and the values will be used for the comparison of the seven indoles investigated in the present work.

Table II. The Apparent Phosphorescence Lifetimes,<sup>a</sup> the Relative Luminescence Yields Relative to Indole, in EPA at  $77^\circ\text{K}$ , and the Ratios of the Phosphorescence to Fluorescence Yields

Compound	$\tau_p$	$\phi_f$	$\phi_p$	$\phi_p/\phi_f$
Indole	$6.0 \pm 0.2$	1.00	1.00	0.37
Indole-3-acetic acid	5.8	0.87	0.75	0.33
Indole-N-acetic acid	5.4	0.78	0.65	0.31
Indole-2-carboxylic acid	1.9	0.91	0.35	0.14
Indole-3-carboxylic acid	4.8	0.80	1.14	0.53
Indole-5-carboxylic acid	5.1	0.38	1.51	1.49
Indole-3-aldehyde	0.6	0.07	1.75	10.00

<sup>a</sup> In seconds.

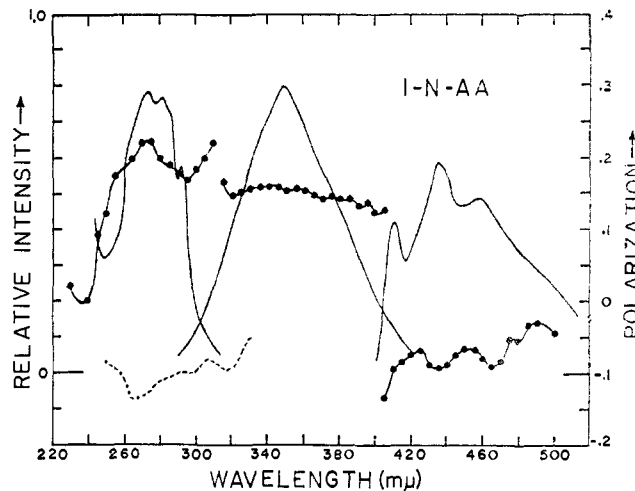


Figure 3. The absorption, emission, and polarization spectra of indole-N-acetic acid. See Figure 1 for legends.

The absorption, emission, and corresponding polarization spectra of indole-3-acetic acid are given in Figure 2. As is readily apparent and qualitatively predictable, the spectra are almost identical with those of indole in Figure 1. However, the degree of the fluorescence polarization of indole-3-acetic acid is somewhat higher than that of indole. In addition to the molecular weight effect on the rotational relaxation time of the molecule, a possible explanation for the increase in the degree of the fluorescence polarization is that the excitation band in the  $285\text{-m}\mu$  region contains more  $^1L_a$  component than in indole. This explanation also seems to be consistent with the fact that the phosphorescence emission polarization monitored by exciting the same spectral region ( $290\text{ m}\mu$ ) as in indole is generally more negative than in indole over the phosphorescence emission bands. Otherwise, the spectral features of the two indole molecules are very similar. Although the vibrational structure in the phosphorescence polarization spectrum of indole-3-acetic acid is not as clearly resolved as in indole, the two polarization spectra closely parallel one another. We conclude, therefore, that the spectral assignments of the fluorescent ( $^1L_a$ ) and phosphorescent states ( $^3L_a$ ) are the same as in indole. However, there are some differences between the two molecules, revealing the effects of the substituent. As shown in Table II, the phosphorescence lifetime of indole-3-acetic acid is nearly the same as in indole, but the relative ratio of the phosphorescence to fluorescence yields is smaller for indole-3-acetic acid than for indole. This is due to the fact that the relative phosphorescence and fluorescence yields are smaller for indole-3-acetic acid than for indole either in solution or in an EPA glass. The absolute fluorescence quantum yields of neutral indole-3-acetic acid and indole in water at room temperature are  $0.307$  and  $0.460$ , respectively.<sup>38</sup> Tryptophan (indole-3-alanine) has also been studied spectroscopically. Its fluorescence spectra were reported by Weber<sup>29</sup> and Konev,<sup>39</sup> and are similar to those presented in Figure 2 for indole-3-acetic acid.

Figure 3 shows the spectra for indole-N-acetic acid. Table II also contains the luminescence ratio and life-

(38) J. W. Bridges and R. T. Williams, *Biochem. J.*, **107**, 225 (1968).

(39) Reference 5, pp 9-21.

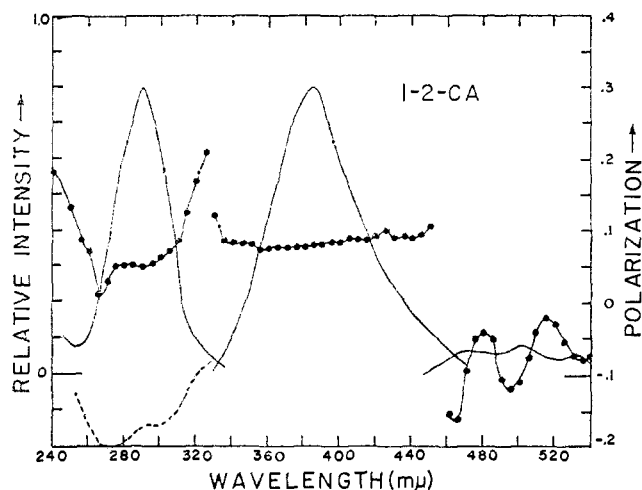


Figure 4. The absorption, emission, and polarization spectra of indole-2-carboxylic acid. See Figure 1 for legends.

time for this molecule. The substitution at the pyrrolic nitrogen of the indole ring is not expected to perturb the molecule to a significant extent. As can be seen, the spectral characteristics very closely resemble the case of indole itself. The phosphorescence lifetime is slightly shorter than that of indole. The most sensitive quantity with respect to substitutions appears to be the relative luminescence yield, as illustrated in Table II. In this respect, indole-N-acetic acid closely resembles indole-3-acetic acid. We therefore assign  $^1L_a$  and  $^3L_a$  to the fluorescent and phosphorescent states of this molecule, based on the resemblance of the degree of polarization and the vibrational activity in the phosphorescence polarization of this compound to the corresponding quantities in indole. When we designate the fluorescent states of indoles as  $^1L_a$ , we do not imply that dual emission from the  $^1L_b$  states is ruled out here. What is meant is that the polarized fluorescence spectra beyond the 0-0 region (where considerably higher degrees of polarization are seen) represent predominantly  $^1L_a$  character. In fact, however, dual emission has been found in most of the indoles and will be commented on in the Discussion section.

Figure 4 contains the results for indole-2-carboxylic acid. We begin to see noticeable differences here, and these differences may be due to the fact that the carboxyl group is now directly conjugated with the indole ring. First of all, the absorption spectrum has lost the long-wavelength shoulder and some of the structure present in the indole spectrum. In fact, the absorption spectrum has become a broad band similar in shape to the fluorescence emission band. The maximum absorption is at 292  $m\mu$ , and the  $^1L_b$  band is now buried under the  $^1L_a$  envelope. It should also be noted that the fluorescence emission is slightly less polarized than in indole, with some increase in the degree of polarization in the longer wavelength region. With most of the other indoles, the degree of polarization tends to decrease with wavelength. It can reasonably be assumed that such a peculiarity in the polarization spectrum is perhaps associated with the fact that the excitation at 305  $m\mu$  equally involves both the  $^1L_a$  and  $^1L_b$  bands. The fluorescence excitation polarization in the region of the maximum absorption is very low, and the minimum corresponding to the  $^1L_b$  band has all

but disappeared. All the spectra of indole-2-carboxylic acid have been red shifted as compared to the spectra of indole and indole-3-acetic acid. In addition, the relative luminescence ratio and the phosphorescence lifetime in Table II indicate a strong perturbation of the indole states and the electronic relaxation processes of the indole ring by the 2-carboxyl substituent. The phosphorescence of indole-2-carboxylic acid is much the same as for the other indoles in that it is broad, with some trace of vibrational structure. As can be seen from Table II, the phosphorescence and the relative luminescence yield of this compound are rather low. The phosphorescence band is negatively polarized with respect to the 305- $m\mu$  excitation oscillator. The two vibrational sequences observed in indole also seem to be present in the phosphorescence polarization spectra of this compound: namely, those of maximum polarization at 480  $m\mu$  ( $20,840\text{ cm}^{-1}$ ;  $1 \times 660\text{ cm}^{-1}$ ) and 515  $m\mu$  ( $19,450\text{ cm}^{-1}$ ;  $ca. 2 \times 660\text{ cm}^{-1}$ ), and those of minimum polarization at 496  $m\mu$  ( $20,150\text{ cm}^{-1}$ ;  $1 \times 1400\text{ cm}^{-1}$ ) and 535  $m\mu$  ( $18,700\text{ cm}^{-1}$ ;  $ca. 2 \times 1400\text{ cm}^{-1}$ ). We can thus reasonably assign  $^3L_a$  as the phosphorescent state of indole-2-carboxylic acid. However, in view of the peculiar fluorescence polarization spectrum of this molecule (Figure 4), one cannot as easily assign  $^1L_a$  to the fluorescent state in analogy with the indole case. This point will be discussed later.

The spectra for indole-3-carboxylic acid are shown in Figure 5. The absorption spectrum is very similar to indole's. The fluorescence excitation polarization spectrum, though it has a shape similar to that of indole's, is more positively polarized in the region where  $^1L_a$  and  $^1L_b$  both absorb, with the magnitude of the former apparently being dominant. The minimum at 230  $m\mu$  is actually negative in this case, indicating that this transition is nearly perpendicular to  $^1L_a$ . However, the phosphorescence polarization beyond the 0-0 band (400  $m\mu$ ) is close to zero, if the polarization spectrum is monitored with the 295- $m\mu$  excitation band. The 0-0 band is still negative ( $-0.07$ ), indicating a perpendicular orientation of the triplet-singlet oscillator with respect to the molecular plane. The near-zero phosphorescence emission polarization is also confirmed by the increasing polarization in the long-wavelength end of the phosphorescence excitation spectrum, as shown in Figure 5. Although the phosphorescence emission polarization spectrum is not as clearly resolved as in indole, the essential feature of the indole spectrum (*i.e.*, the two series of vibrations with alternating degrees of polarization) also appears to be present in indole-3-carboxylic acid. Therefore, one can reasonably assign the two luminescent states of indole-3-carboxylic acid to the same species as in indole and indole-3-acetic acid. The phosphorescence lifetime is now significantly decreased (Table II), and the relative fluorescence yield is considerably lower than that of indole-3-acetic acid and indole. However, the relative luminescence ratio is not too different from that of indole-3-acetic acid. In fact, the relative phosphorescence yield of indole-3-carboxylic acid is significantly higher than that of indole or indole-3-acetic acid. This suggests rather efficient radiationless transitions (excluding intersystem crossing) to the ground state in the singlet manifold, thus lowering  $\phi_F$  relative to indole.

In the case of indole-5-carboxylic acid, the data for

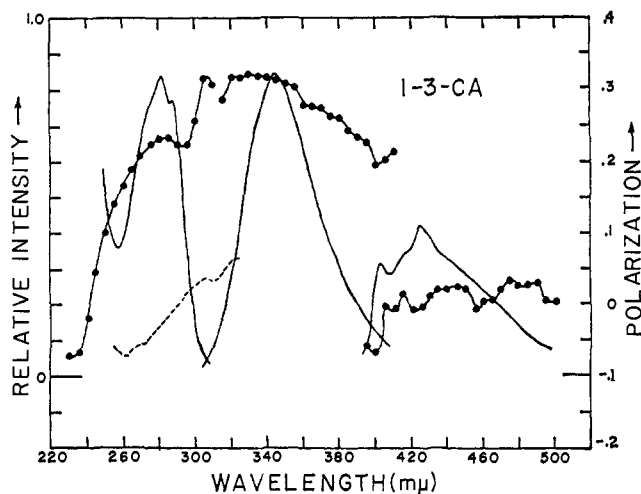


Figure 5. The absorption, emission, and polarization spectra of indole-3-carboxylic acid. See Figure 1 for legends.

which are seen in Figure 6, the absorption and fluorescence spectra can be described qualitatively in the same terms as the indole-2-carboxylic acid spectra (Figure 4). The fluorescence spectrum in EPA at 298°K is also presented here. The Stokes and  $\lambda_{\text{max}}^f$  shifts for fluorescence in methanol are large and the fluorescence emission appears to be partially enveloped by the phosphorescence spectrum. This of course is not the case for the fluorescence spectrum in EPA. In this respect, indole-5-carboxylic acid is most unique. The absorption spectrum has lost its structure completely, and the  $^1L_b$  band (ca. 304  $m\mu$ ) is apparently hidden under the  $^1L_a$  envelope. The polarized fluorescence emission and excitation spectra are very similar to those of indole-2-carboxylic acid. It is to be noticed that the long-wavelength region of the fluorescence spectrum has gradually increasing degrees of polarization, unlike most of the other indoles. Actually, the fluorescence emission spectrum beyond the 0-0 band is almost completely depolarized. Nevertheless, it is readily apparent that the 0-0 absorption at 335  $m\mu$  and the 0-0 fluorescence emission at about 338-340  $m\mu$  are polarized in a manner analogous to the other indoles presented in Figures 1-5, thus enabling us to assign the 0-0 fluorescence to  $^1L_b$  (see Discussion). Thus,  $^1L_b$  is also involved in the emission. The thermal equilibrium between the  $^1L_a$  and  $^1L_b$  levels in the fluorescent state may also depolarize the spectrum. This aspect will be more thoroughly discussed later. The triplet-singlet emission is not structured as with the previous cases, and this is further confirmed by the near structureless emission polarization spectrum. The degree of polarization of the 0-0 phosphorescence emission band at 405  $m\mu$  is negative, and the lifetime was 5.1 sec (Table II), so the emission apparently occurs from  $^3L_a$ . The vibrational structure is no longer apparent in this molecule, and the degree of polarization beyond the 0-0 phosphorescence band is also nearly zero. It is clear that the phosphorescence excitation at the long-wavelength end of the absorption spectrum is definitely polarized perpendicular to the triplet-singlet oscillator. The relative luminescence ratio (phosphorescence over fluorescence) for this molecule was found to be larger than unity, indicating that intersystem crossing is rather efficient here. This is reflected by the fact that the

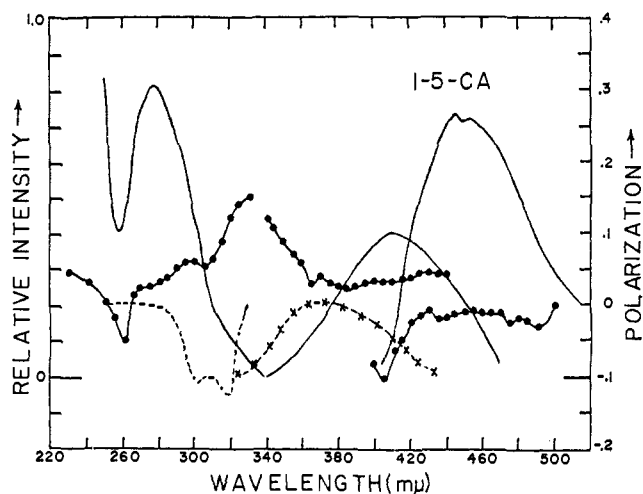


Figure 6. The absorption, emission, and polarization spectra of indole-5-carboxylic acid. See Figure 1 for legends.

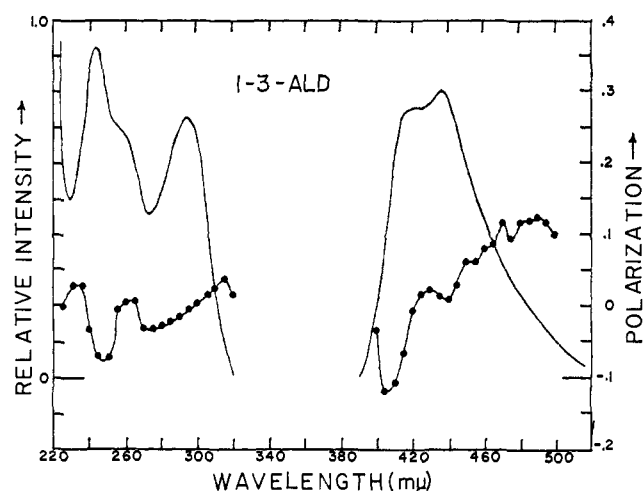


Figure 7. On the left: the absorption (—) and polarized phosphorescence excitation (●) spectra of indole-3-aldehyde. On the right: the phosphorescence emission (—) and polarized phosphorescence emission (●) spectra. The weak fluorescence emission spectrum with maximum  $\lambda^f$  at 355  $m\mu$  is not recorded here. See Figure 1 for further legends.

relative phosphorescence yield in indole-5-carboxylic acid is larger than any of the indoles described so far.

One other molecule which shows a relative luminescence ratio larger than unity is indole-3-aldehyde, and the data for this molecule are presented in Figure 7 and Table II. Indole-3-aldehyde is also known to be one of the photoproducts in the phototropic reaction involving riboflavin and indole-3-acetic acid.<sup>40</sup> We were able to obtain only an extremely weak fluorescence from this compound, and the phosphorescence was much more intense than for indole (Table II). The formaldehyde substitution at position 3 has altered the absorption spectrum of indole-3-aldehyde from that of indole in the following two ways: (a) the long-wavelength shoulder characteristic of indole has disappeared, thus burying the  $^1L_b$  band under the intense  $^1L_a$  band; (b) the spectrum is red shifted, with the appearance of a shoulder in the 260- $m\mu$  region. The phosphorescence emission spectrum is the most unique among the indole derivatives considered. As can be seen from Figure 7,

(40) B. Nathanson, M. Brody, S. Brody, and S. B. Brody, *Photochem. Photobiol.*, 6, 177 (1967).

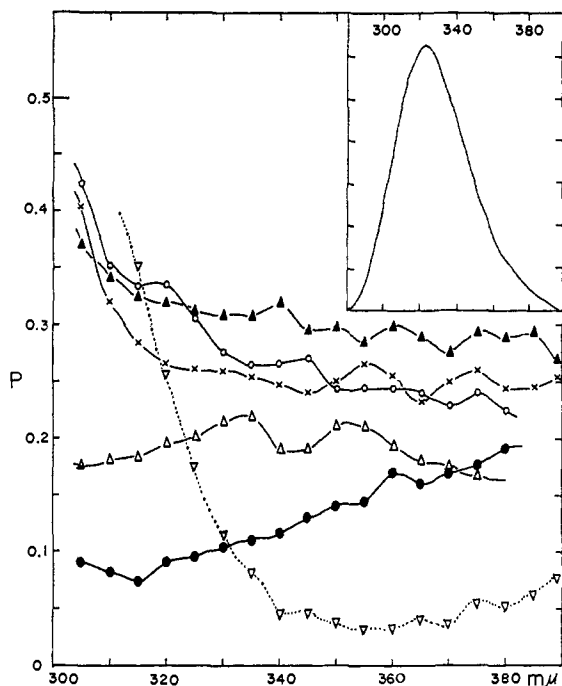


Figure 8. The polarized fluorescence emission spectra of the indoles (*ca.*  $10^{-5}$  *M*) in EPA at 77°K: ×, indole; ▲, indole-3-acetic acid; △, indole-N-acetic acid; ●, indole-2-carboxylic acid; ○, indole-3-carboxylic acid; and ▽, indole-5-carboxylic acid. The fluorescence emission spectrum of indole in EPA at 77°K is also inserted in the upper right-hand corner of the figure.

the entire emission band beyond the negatively polarized 0-0 band is positively polarized, with positively polarized vibronic structure appearing in the polarization spectrum. The phosphorescence excitation spectrum is also unique, in that the apparent 0-0 absorption is positively polarized (*ca.* +0.05). It can be concluded that the electric dipole allowed phosphorescence oscillator (0-0 band) is perpendicular to the excitation oscillator(s) at 300  $m\mu$ , but significant intensity from the plane-polarized singlet-singlet transition moments ( $^1L_a$ ,  $^1L_b$ , and the shoulder at 260  $m\mu$ ) has also been stolen by the triplet-singlet transition. The lifetime, 0.6 sec, is still long enough to be characteristic of a  $^3(\pi, \pi^*)$  emitter,<sup>41</sup> and thus the assignment of  $^3L_a$  for the phosphorescent state of indole-3-aldehyde. The possible role of  $^1,^3(n, \pi^*)$  states in the spectroscopy and electronic relaxation process of this molecule will be discussed later. Finally, it is reemphasized that the relative phosphorescence and luminescence ratio of indole-3-aldehyde are the highest among the seven indoles studied, as can be seen from Table II.

**2. Polarized Fluorescence Emission Spectra in EPA at 77°K.** The fluorescence polarization spectra presented in Figures 1-7 were obtained in polar solvents (glycerol-methanol, 9:1) at 263°K in order to minimize Brownian rotary depolarization. In addition, we overcame earlier instrumental difficulties in obtaining accurate polarizations of the indole fluorescence in EPA glass at 77°K. The polarized fluorescence spectra were obtained by measuring the degree of polarization of the sample in a phosphorescence dewar, and by correcting for scattering effects as well as for other instrumental depolarizing factors by using two exciting

(41) L. Vanquickenborne and S. P. McGlynn, *J. Chem. Phys.*, **45**, 4755 (1966).

and two analyzing polarizers, as described in the Experimental Section. The results are presented in Figure 8. Figure 8 contains a typical fluorescence emission spectrum of indole and the fluorescence polarization spectra of six indoles in EPA at 77°K. The polarized emission spectrum of indole-3-aldehyde is not included in Figure 8, because of the difficulty in obtaining a reliable polarization spectrum of this very weakly fluorescent compound. The emission spectra in EPA at 77°K are blue shifted approximately 25-30  $m\mu$  relative to their corresponding spectra in glycerol-methanol (9:1) at 263°K. The degree of polarization is significantly increased in EPA at low temperature, as a result of nonpolar solvent effects on the emission spectra and an almost complete restriction of molecular rotation in the rigid matrix. Nevertheless, it is apparent that the spectral characteristics of most of the indoles are not markedly altered in the low-temperature EPA matrix, relative to their spectra in a polar solvent at 263°K. In the case of indole-2-carboxylic acid and indole-5-carboxylic acid, the increase in polarization in the longer wavelength region of the fluorescence emission spectra is much more pronounced at 77°K than at 263°K. This confirms the unusual behavior of these two indoles in their polarization dependence on the emission wavelength described in connection with Figures 4 and 6. It is interesting to note that the theoretical maximum polarization of 0.5, for the photoselection of nonsymmetric molecules, was not obtained for any of the indoles shown in Figure 8. We believe this is due to the inherent difficulty in isolating the purely monochromatic  $^1L_a$  and  $^1L_b$  bands for the polarization measurements, with a resultant lowering of the degree of polarization of these indoles. An additional factor in the inability to attain the value of 0.5 is that the conditions for obtaining the theoretical maximum degree of polarization (*i.e.*, polarization measured at the frequency of the 0-0 emission and the frequency of the 0-0 excitation of a pure electronic oscillator) are extremely difficult to meet in low-resolution measurements. In any case, the data presented in Figure 8 definitely supplement the results previously described.

**3. Molecular Orbital Calculations of the Excited States of Indoles.** Table III summarizes the results of the P-P-P SCF MO-CI calculations of the four lowest transition energies both in the singlet and triplet manifolds. The oscillator strengths for the singlet-singlet transitions ( $\pi \rightarrow \pi^*$  type) are also computed and listed in the table. The results are in satisfactory agreement with the experimental energies. The oscillator strengths are considerably lower for  $^1L_b$  than for  $^1L_a$ , and this is also consistent with well-known theoretical and experimental intensity data on the  $^1L_b$  and  $^1L_a$  bands in naphthalene (isoelectronic with indole) and other aromatic hydrocarbons.<sup>42,43</sup> The Platt notations were assigned on the basis of the form of the molecular orbitals<sup>44</sup> and in analogy with Platt's classification of naphthalene.<sup>12,42</sup> It is clear that none of the substituents in

(42) H. B. Klevens and J. R. Platt, *ibid.*, **17**, 470 (1949).

(43) J. N. Murrell, "The Theory of Electronic Spectra of Organic Molecules," John Wiley & Sons, New York, N. Y., 1963, Chapter 6, and references therein.

(44) The details of the theoretical calculations (P-P-P and CNDO MO's) of the electronic structures of ground- and excited-state indoles will be prepared for publication in the near future. The symmetry of the HOMO's and LEMO's of the indole ring was found to be exactly the same, regardless of the substituent or its position.

**Table III.** The Experimental and Calculated  $^1(\pi \rightarrow \pi^*)$  and  $^3(\pi \rightarrow \pi^*)$  Energies of the Indole Derivatives<sup>a</sup>

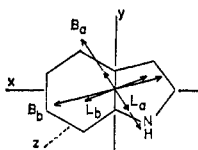
Compound	Configuration	State symbols	$^1(\pi \rightarrow \pi^*)$ , eV (m $\mu$ )			$^3(\pi \rightarrow \pi^*)$ , eV (m $\mu$ )		
			Calcd	<i>f</i>	Obsd <sup>b</sup>	Calcd	Obsd <sup>c</sup>	Obsd <sup>d</sup>
Indole	4 $\rightarrow$ 6	L <sub>b</sub>	4.480 (277)	0.05	4.234 (293)	3.903 (318)		
	5 $\rightarrow$ 6	L <sub>a</sub>	4.966 (250)	0.19	4.643 (267)	2.190 (566)	2.856 (433)	2.848 (435)
	4 $\rightarrow$ 7	B <sub>a</sub>	6.337 (196)	1.19				
	5 $\rightarrow$ 7	B <sub>b</sub>	5.953 (208)	0.70	5.635 <sup>e</sup> (220)			
Indole-3-acetic acid	7 $\rightarrow$ 9	L <sub>b</sub>	4.668 (266)	0.08	4.246 (292)	3.671 (338)		
	8 $\rightarrow$ 9	L <sub>a</sub>	4.353 (285)	0.12	4.587 (270)	2.334 (531)	2.821 (440)	2.821 (440)
	7 $\rightarrow$ 10	B <sub>a</sub>	6.500 (191)	0.02				
Indole-N-acetic acid	8 $\rightarrow$ 10	B <sub>b</sub>	5.156 (240)	0.01	5.393 (230)			
	7 $\rightarrow$ 9	L <sub>b</sub>	4.434 (280)	0.08	4.228 (293)	3.658 (339)		
	8 $\rightarrow$ 9	L <sub>a</sub>	4.942 (251)	0.19	4.550 (272)	2.361 (525)	2.821 (440)	2.856 (434)
	7 $\rightarrow$ 10	B <sub>a</sub>	6.033 (206)	0.15				
Indole-2-carboxylic acid	8 $\rightarrow$ 10	B <sub>b</sub>	5.874 (211)	0.03	5.337 (232)			
	6 $\rightarrow$ 8	L <sub>b</sub>	4.246 (292)	0.09	4.270 (290)	3.106 (399)		
	7 $\rightarrow$ 8	L <sub>a</sub>	4.540 (273)	0.064	4.507 (275)	2.003 (619)	2.480 (500)	2.480 (500)
	6 $\rightarrow$ 9	B <sub>a</sub>	5.688 (218)	0.01				
Indole-3-carboxylic acid	7 $\rightarrow$ 9	B <sub>b</sub>	5.420 (229)	0.68				
	6 $\rightarrow$ 8	L <sub>b</sub>	4.460 (278)	0.07	4.246 (292)	3.922 (316)		
	7 $\rightarrow$ 8	L <sub>a</sub>	4.720 (263)	0.28	4.408 (281)	2.156 (575)	2.920 (425)	2.920 (425)
	6 $\rightarrow$ 9	B <sub>a</sub>	5.656 (219)	0.39				
Indole-5-carboxylic acid	7 $\rightarrow$ 9	B <sub>b</sub>	5.531 (224)	0.39	5.393 (230)			
	6 $\rightarrow$ 8	L <sub>b</sub>	4.285 (289)	0.01	4.079 (304)	4.095 (303)		
	7 $\rightarrow$ 8	L <sub>a</sub>	4.694 (264)	0.08	4.476 (277)	2.177 (569)	2.783 (445)	2.783 (445)
	6 $\rightarrow$ 9	B <sub>a</sub>	5.642 (220)	0.43				
Indole-3-aldehyde	7 $\rightarrow$ 0	B <sub>b</sub>	5.418 (229)	1.53	5.400 (230)			
	5 $\rightarrow$ 7	L <sub>b</sub>	4.446 (279)	0.08	<i>d</i>	3.470 (377)		
	6 $\rightarrow$ 7	L <sub>a</sub>	4.637 (267)	0.31	<i>d</i>	2.188 (567)	2.857 (434)	2.838 (436)
	5 $\rightarrow$ 8	B <sub>a</sub>	5.490 (226)	0.13	<i>d</i>			
	6 $\rightarrow$ 8	B <sub>b</sub>	5.484 (226)	0.56	<i>d</i>			

<sup>a</sup> The calculated values were obtained by the P-P-P SCF MO-CI method. The oscillator strengths (*f*) for the singlet-singlet transitions are also given. <sup>b</sup> From the polarized fluorescence excitation spectra whenever possible. Otherwise, absorption spectra were used for these values. More accurate values are yet to be obtained from higher resolution measurements. <sup>c</sup> From ref 31. <sup>d</sup> Due to lack of sufficient fluorescence emission from this molecule, the polarized fluorescence excitation spectrum was not obtainable, thus making it difficult to interpret the absorption spectrum (Figure 7), particularly in the region 230–270 m $\mu$ . <sup>e</sup> Corrected phosphorescence maxima. <sup>f</sup> Uncorrected phosphorescence maxima.

the indoles studied perturbs the system sufficiently to make  $^1L_a$  the lowest singlet state (under Franck-Condon conditions). The anomaly in indole-3-acetic acid, *i.e.*, the reversal of the calculated  $^1L_a$  and  $^1L_b$  energies, will be discussed later. However, the oscillator strengths are predicted to be rather sensitive to the substituents. These calculated results will be used to interpret the experimental data in the Discussion section.

Figure 9 shows the calculated polarizations of the four lowest transition moments as well as the experimental orientations (relative) of the  $^1L_b$  and  $^1L_a$  moments. The agreement is surprisingly good, within experimental errors and the theoretical approximations. The combination of the calculated direction (absolute) and observed orientation (relative) of the singlet-singlet transition moments is helpful in describing the





	POLARIZATION				$\theta'$	
	$L_b$	$L_a$	$B_a$	$B_b$	CALC.	OBS.
(I) Indole	x	y	y	x	78°	90°
I-3-acetic acid	x	y	y	x	83	87
I-N- " "	x	y	y	x	80	81
I-2-carboxylic "	x	y	y	x	64	76
I-3- " "	x	y	y	x	89	78
I-5- " "	x	y	y	x	75	77
I-3-aldehyde	x	y	y	x	83	?

Figure 9. The calculated polarizations of the single-singlet ( $\pi \rightarrow \pi^*$ ) transitions in indoles. The coordinate designation and a typical diagram for the transition moments are given for indole as the reference molecule. The mutual orientation angles ( $\theta'$ ) between the  $L_b$  and  $L_a$  moments are listed in the last two columns.

electronic states studied in Figures 1-7.  ${}^1L_b$  is predicted to be nearly long-axis polarized in all cases, analogous to the naphthalene case.<sup>12</sup> Finally, we will comment on the method of estimating the "observed" relative orientation angle ( $\theta'$ ) in Figure 9 from the fluorescence polarization data. First, the angle  $\theta$  between the emitting oscillator and a given exciting oscillator ( ${}^1L_b$  and  ${}^1L_a$ ) was calculated from Figures 1-7 by means of the Levshin-Perrin formula<sup>45,46</sup>

$$P = \frac{3 \cos^2 \theta - 1}{\cos^2 \theta + 3}$$

Then,  $\theta'$  was calculated from the two values of  $\theta$ . Due to depolarizations and other possible experimental errors (e.g., temperature variations from one measurement to another),  $\theta'$  estimated in this manner is not completely "quantitative." However, it was also found that limited depolarizations did not markedly affect the estimated  $\theta'$  values. Only the angle between the two lowest transition moments is given in Figure 9 because the polarization was not resolved in the short-wavelength region. However, the calculation predicts that there is a large angle between the two short-wavelength bands ( $B_a$  and  $B_b$ ) and this is apparently confirmed, at least in one case, as seen in the spectrum of indole-2-carboxylic acid (Figure 4).

As is usually the case with P-P-P calculations of open-shell configurations, the calculated singlet-triplet transition energies are considerably lower than the experimental values. This lack of even qualitative agreement between the calculated and observed triplet energies is mainly due to the fact that semiempirical integrals such as the one-electron core Hamiltonian matrix elements ( $\beta^{\text{core}}$ ) and the one- and two-center electron interaction integrals were evaluated with reference to the singlet-singlet transition energies of closed shell systems. Furthermore, the triplet energies are very sensitive to the number of configurations in the CI treatment, unlike singlet-singlet transition energies. Therefore, the singlet-triplet energies listed in Table III are not very meaningful. However, one aspect of the calculated data is undoubtedly significant, and that is that

(45) V. L. Levshin, *Z. Phys.*, **32**, 307 (1925).

(46) F. Perrin, *Ann. Phys.*, **12**, 169 (1929).

the lowest triplets of all the indole molecules calculated are of  ${}^3L_a$  type.

## Discussion

**1.  $S_0 \leftrightarrow S$  Transitions.** It is apparent that the  ${}^1L_a$  state is the predominant fluorescent state in most of the indoles studied, and the 0-0  ${}^1L_a$  absorption bands are in the long-wavelength end of the absorption and fluorescence excitation spectra. Since the Franck-Condon allowed  ${}^1L_b$  band appears between the intense  ${}^1L_a$  and its 0-0 band the description of the potential energy surfaces of most of the indoles presently studied fits well with the potential surfaces suggested by Weber for indole.<sup>23</sup> Such a situation is well known for other systems such as naphthalene in which the  ${}^1L_b$  band appears, at longer wavelengths than the vertical excitation band of  ${}^1L_a$ .<sup>42,43</sup> Our calculations (Table III and Figure 9) are consistent with this description. We have used Platt notation to classify the electronic bands of the various indoles in Table III on the basis of a spectroscopic correlation of indole and naphthalene.<sup>12</sup> The theoretical correlation of the forms of the molecular orbitals in indole with those of naphthalene ( $D_{2h}$ ) has recently been done with reasonable success.<sup>47</sup> Momicchioli and his coworker<sup>47</sup> used only four singly excited configurations in their P-P-P SCF MO-CI calculation of indole, but their results on energies and polarizations are in reasonable agreement with our data on indole, as shown in Table III and Figure 9, in which we employed a considerably larger number of configurations. Konev and his coworker<sup>30</sup> have studied the fluorescence polarization of indole in stretched PVA films in which the molecules are forced to orient in a preferred direction. They resolved three bands:  ${}^1L_b$  at 289 m $\mu$ ,  ${}^1L_a$  at 266 m $\mu$ , and  ${}^1B_b$  at 220 m $\mu$ . Their assignments and polarizations are confirmed in the present work (see Figures 1 and 9, Table III) on indole.

In Table III,  ${}^1L_a$  is lower than  ${}^1L_b$  in the calculation of indole-3-acetic acid. This is not consistent with the absorption spectrum and the polarized fluorescence emission and excitation spectra of this molecule (Figure 2), although the polarizations, as shown in Figure 9, are apparently in agreement with the experimental data. The calculated energy reversal and the extremely weak calculated intensities in this compound are probably due to the inappropriate integrals used in treating the methylene bridge as a hyperconjugating group orbital. Further theoretical investigations of the treatment of methyl and methylene groups in molecular orbital calculations are warranted.

We now turn to the question of dual emission in indole and its derivatives. Zimmermann and his coworkers<sup>13,48</sup> suggested the emission from both  ${}^1L_a$  and  ${}^1L_b$  states on the basis of fluorescence polarization data. Such a dual emission may be possible due to thermal equilibration between the singlet excited states ( ${}^1L_a$  and  ${}^1L_b$  zero vibrational levels). It is also possible if radiationless transition  $S_2 \rightarrow S_1$  is strongly hindered.<sup>48,49</sup> Mataga, *et al.*,<sup>50</sup> measured the fluorescence decay curve

(47) F. Momicchioli and A. Rastelli, *J. Mol. Spectry.*, **22**, 310 (1967).

(48) H. Zimmermann and N. Joop, *Ber. Bunsenges. Physik Chem.*, **65**, 61 (1961).

(49) V. P. Klochkow and B. S. Neporent, *Opt. Spectry.*, **12**, 125 (1962).

(50) N. Mataga, Y. Torihashi, and K. Ezumi, *Theoret. Chim. Acta*, **2**, 158 (1964).

of indole in cyclohexane and acetonitrile by using a uv light pulse excitation of very short duration. Two components (long decay component,  ${}^1L_b$ , and short component,  ${}^1L_a$ ) were detected in the emission bands. However, the short component was predominant in polar solvent. Konev, *et al.*,<sup>34</sup> carried out a vibrational analysis of indole fluorescence in cyclohexane at 77°K, also confirming the dual emission. Other workers<sup>32,51</sup> have also confirmed the dual emission from indole in cyclohexane. It was found that the fluorescence polarization in glycerol was constant along the emission band, indicating that the emission was predominantly from  ${}^1L_a$ . With the possible exception of indole-N-acetic acid (Figures 3 and 8), dual emission in most of the indoles investigated appears to be very likely on the basis of the sharp changes in the degree of polarization of the fluorescence emission in the short-wavelength region, followed by the gradual decrease in the long-wavelength region (Figures 1, 2, 4, 5, 6, and 7). The sharp increase in the short-wavelength end of the fluorescence polarization is most likely associated with the apparent 0-0 emission (or Franck-Condon allowed transition from the zero vibrational level to a vibrational level of the ground electronic state) of  ${}^1L_b$ , which is oriented parallel with respect to the exciting moment at 285–305  $m\mu$  (rich in  ${}^1L_b$  components). The gradual decrease in the degree of the fluorescence polarization at longer wavelengths can be associated with the emission from  ${}^1L_a$  as well as some vibronic activity due to depolarizing non-totally symmetric vibrations. On the basis of these observations, it is apparent that the dual emission indeed appears to occur in most of the indoles studied, even in polar solvents (glycerol-methanol in our case). Therefore, our results confirm the suggestions by Zimmermann and his coworkers,<sup>13,48</sup> who examined the fluorescence emission from indole in ethanol at 77°K. In addition, we have now demonstrated that the dual emission in various indoles seems to be of common (if not general) occurrence. The dual emission can be further examined by (a) measuring the fluorescence polarization in nonpolar solvents at low temperatures and by (b) monitoring the polarized emission by exciting with 265- $m\mu$  (rich in  ${}^1L_a$ ) light. This has been done, and the results are shown in Figures 8 and 10. The dual emission is favored if the Stokes shift is small, so that the  $S_1$  and  $S_2$  states are closely spaced. This is revealed by comparing the spectral positions of indole and indole-5-carboxylic acid in a polar solvent (Figure 1 and Figure 6, respectively) with those in an EPA (nonpolar) glass (Figure 6 and Figure 8, respectively). This shift can readily be understood from the fact that the dipole moment of  ${}^1L_a$  is larger than that of  ${}^1L_b$ ,<sup>50</sup> as also predicted by our calculations.<sup>44</sup> Figure 8 shows the polarized fluorescence spectra of the indoles in EPA at 77°K. It is apparent that the spectrum at the short-wavelength end shows a considerably higher degree of polarization than at the longer wavelength end (*i.e.*, for indole, indole-3-acetic acid, indole-3-carboxylic acid, and indole-5-carboxylic acid), again demonstrating the dual emission. It is not possible from our experiments to estimate the relative contributions of  ${}^1L_a$  and  ${}^1L_b$  to the emission, although the  ${}^1L_a$  components prevail throughout the longer wavelength region. This

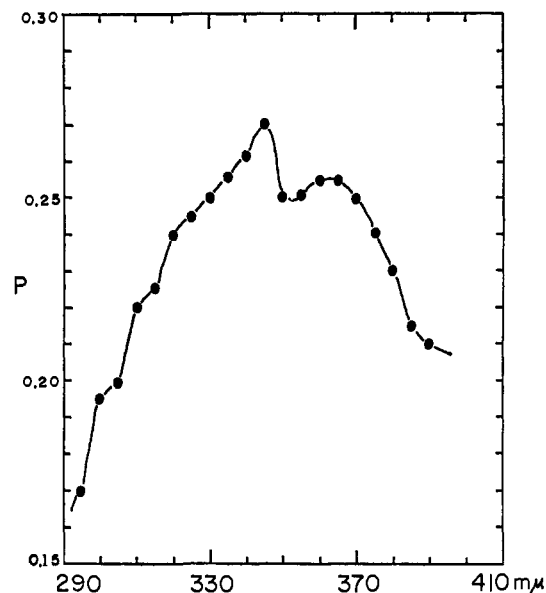


Figure 10. The polarized fluorescence emission spectrum of indole ( $10^{-5} M$ ) in EPA at 77°K. The degree of polarization was measured by monitoring the excitation at 265  $m\mu$ , which is rich in  ${}^1L_a$  components.

is because of the fact that the excitation is not really of pure  ${}^1L_b$  because of its overlap with the  ${}^1L_a$  band in most of the indoles. In addition, the dual emission will result in depolarization if both  ${}^1L_a$  and  ${}^1L_b$  emit throughout the emission bands. In order to further examine the nature of the dual emission and the polarization of the 0-0 emission bands of the indoles, indole was chosen as a representative molecule and its polarized emission was obtained using 265- $m\mu$  excitation in which  ${}^1L_a$  is the major component. Figure 10 shows the results. The emission polarization at the short-wavelength end of indole in EPA at 77°K is now opposite to that obtained by 285  $m\mu$  or 292  $m\mu$   ${}^1L_b$ -rich excitation (Figures 1 and 8, respectively). This suggests that the emission oscillator in this region is oriented approximately perpendicular to the  ${}^1L_a$  excitation moment, while the higher degree of polarization at longer wavelengths is obviously associated with a parallel orientation between the emission and excitation transition moments ( ${}^1L_a$ ). This conclusively supports the occurrence of the dual emission in indoles deduced from the fluorescence polarization data shown in Figures 1-8. In order to further verify the dual emission, we have carried out preliminary measurements of the polarized fluorescence excitation spectrum of indole in EPA at 77°K by monitoring the emission at 300  $m\mu$  (supposedly rich in the  ${}^1L_b$  component if the dual emission is operative) and at 340  $m\mu$  (rich in  ${}^1L_a$ ). The degree of the excitation polarization at 282–290  $m\mu$  ( ${}^1L_b$ ) is minimum (0.21) with respect to the 340- $m\mu$  ( ${}^1L_a$ ) emission, while the same excitation band becomes considerably more polarized (0.42–0.47) with the emission at 300  $m\mu$  ( ${}^1L_b$ ). The  ${}^1L_a$  excitation band region now becomes minimum in the latter case (emission at 300  $m\mu$ ). These results definitely constitute further proof of the dual emission.

As mentioned earlier, the polarized fluorescence spectrum of indole-2-carboxylic acid is somewhat different from the others in that the degree of polarization increases with wavelength (Figures 4 and 8). This appears to be coupled with the disappearance of the  ${}^1L_b$

(51) V. P. Borbrovich, G. S. Kembrovskii, and N. I. Marenko, *Dokl. Akad. Nauk Beloruss. SSSR*, 10, 936 (1966).

shoulder in the absorption spectrum. In both Figures 4 and 8, the increase in polarization at the short-wavelength end of the fluorescence spectrum is not as apparent as in the other indoles. This can be explained by the fact that excitation at 305 m $\mu$  does not preferentially involve  $^1L_b$  or at least that the  $^1L_b$  band is considerably masked by the overlapping  $^1L_a$  band. This can be deduced from the disappearance of the  $^1L_b$  shoulder and loss of the excitation polarization minimum at this wavelength (Figure 4). Therefore, the increase in the degree of polarization in the fluorescence spectrum at longer wavelengths is most likely associated with emission from  $^1L_a$ , the moment of which is oriented parallel to the excitation moment ( $^1L_a$  rich). This increase is much more evident in Figure 8 than in Figure 4. The apparent decrease, or minimum, at the short-wavelength end of the polarized fluorescence can be associated with the  $^1L_b$  contribution. Thus, the dual emission is also operating in indole-2-carboxylic acid. Indole-5-carboxylic acid seems to behave in the same way as the other indoles (Figures 6 and 8). It is noteworthy that the calculated energy gap between the vertical  $^1L_b$  and  $^1L_a$  levels of these two compounds is approximately 0.5 eV smaller than in the other indoles, as can be seen from Table III. This is of course consistent with the masking of the  $^1L_b$  shoulders by  $^1L_a$  in these molecules.

It appears from Figures 3 and 8 that the dual emission in both polar and nonpolar media is not very important in the case of indole-N-acetic acid. The degree of emission polarization does not exceed 0.2, with no apparent sharp increase in P in the short-wavelength region of the polarized fluorescence spectrum. The reason for this lack of dual emission is not known. However, it is noteworthy that the calculated vertical energy gap between the  $^1L_b$  and  $^1L_a$  states of indole-N-acetic acid is relatively large compared to the other indoles listed in Table III. Whether this is related to a preferential emission from  $^1L_a$  in this molecule cannot be ascertained, because indole-5-carboxylic acid with the largest energy gap clearly shows dual emission (Figures 6 and 8), and agreement with the observed energies is not always seen. Further investigations are obviously needed. It would be helpful to study a variety of indole derivatives in order to correlate the nature of the electronic states with their luminescence behaviors.

**2.  $S_0 \leftrightarrow T$  Transitions.** The phosphorescence spectra of indole and its derivatives, in contrast to the fluorescence spectra, are distinctly structured in most cases (Figures 1–7). The measured lifetimes shown in Table II reflect the ( $\pi, \pi^*$ ) nature of the phosphorescent triplet states. The 0–0 emission bands of all the indole molecules studied (Figures 1–7) are negatively polarized with respect to the excitation wavelengths specified in Table I. According to the spin-orbit coupling selection rules within the framework of the Born–Oppenheimer approximation,<sup>52</sup> one- and two-center spin-orbit coupling matrix elements between singlet and triplet ( $\pi, \pi^*$ ) states in indoles with no available ( $n, \pi^*$ ) states are expected to be very small, and the important spin-orbit coupling term must be that between  $^1(\sigma, \pi^*$  or  $\pi, \sigma^*$ ) and  $^3(\pi, \pi^*)$  states.<sup>53,54</sup>

(52) M. A. El-Sayed, *J. Chem. Phys.*, **38**, 2834 (1963).

(53) S. K. Lower and M. A. El-Sayed, *Chem. Rev.*, **66**, 199 (1966), and references therein.

(54) M. A. El-Sayed, *Acta Physica Polon.*, **34**, 649 (1968).

Since all of the indole molecules presented in Figures 1–7 show negative polarizations in the 0–0 phosphorescence emission region, and the 0–0 emission does not appear to be significantly intense, the mechanism for the singlet–triplet transitions can be identified with direct spin-orbit coupling as predicted with the above selection rules. Obviously, the major intensity contributions (or “intensity stealing”) involve first-order spin vibronic and second-order vibronic spin-orbit couplings,<sup>55,56</sup> as can be deduced from the vibronic activities revealed in the phosphorescence and polarized phosphorescence emission spectra (Figures 1–7). In Figure 1, the maximum and minimum degrees of polarization in the polarized phosphorescence spectrum may be assigned to two series of vibrational modes, a 650 and 1550-cm<sup>-1</sup> series. The former may be correlated with an in-plane skeletal distortion of the indole ring, analogous to that mode found in naphthalene (620-cm<sup>-1</sup>),<sup>57,58</sup> or an out-of-plane C–H bending mode, analogous to that mode in purine. Purine, which is isoelectronic with indole and is a heterocyclic nitrogen analog of indole, shows an out-of-plane C–H bending mode in this region (610–650 cm<sup>-1</sup>).<sup>59</sup> An N–H bending is also a possible mode. The ir spectrum of indole in this region has not been studied. The 1550-cm<sup>-1</sup> series in Figure 1 may be associated with the ring-stretching mode.<sup>60</sup> However, higher resolution studies are needed to confirm our qualitative assignments.

Although the vibronic activities in the other indoles are not resolved, the same kind of vibrational modes are probably involved in some of the polarized phosphorescence spectra of these molecules (e.g., Figures 2, 3, 4, 5, and 6). The assignment of  $^3L_a$  to the phosphorescence band is made based on an analogy to other aromatic hydrocarbons and our theoretical calculations shown in Table III. The  $^3L_a$  assignment can also be deduced from the fluorescence polarization spectra of indoles in which the 0–0 absorption bands are of  $^1L_a$  origin. This, coupled with dominant  $^1L_a$  fluorescence emission at longer wavelengths, warrants the assignment of  $^3L_a$  as the lowest triplet state. Previously, the  $^3L_a$  assignment for the phosphorescent state of naphthalene, which is isoelectronic with indole, was made on the basis of the polarized emission spectra by Czekała, *et al.*,<sup>61</sup> and many others.<sup>62</sup> Konev and his co-worker<sup>6,30</sup> also assigned  $^3L_a$  for indole phosphorescence. However, their results are somewhat different from ours in the following respects: first, they obtained both the fluorescence and phosphorescence polarization spectra of indole in stretched anisotropic films of polyvinyl alcohol. Their degree of fluorescence polarization was nearly constant, and they assigned the fluorescent state to  $^1L_a$ . No dual emission was described. Secondly, they obtained structure in the phosphorescence

(55) A. Albrecht, *J. Chem. Phys.*, **38**, 354 (1963).

(56) R. M. Hochstrasser, “Molecular Aspects of Symmetry,” W. A. Benjamin, Inc., New York, N. Y., 1966, Chapter 9.

(57) W. B. Person, G. C. Pimental, and O. Schnepp, *J. Chem. Phys.*, **23**, 230 (1955).

(58) E. R. Lippincott and E. J. O'Reilly, Jr., *ibid.*, **23**, 238 (1955).

(59) W. C. Coburn, Jr., W. R. Laseter, and C. V. Stephenson, AFOSR-973, Directorate of Chemical Sciences, Air Force Office of Scientific Research, Washington, D. C., 1961.

(60) K. Nakanishi, “Infrared Absorption Spectroscopy,” Holden-Day, Inc., San Francisco, Calif., 1962, p 214.

(61) H.-J. Czekała, W. Liptay, and E. Dollefeld, *Ber. Bunsenges. Phys. Chem.*, **68**, 80 (1964).

(62) For example, R. M. Hochstrasser and S. K. Lower, *J. Chem. Phys.*, **40**, 1041 (1964).

Table IV. The Wave Functions of the  $L_b$  and  $L_a$  Species after Configuration Interaction

Indole	Wave functions
Indole	${}^1\Psi ({}^1L_b) = 0.70L_b + 0.38L_a + 0.18B_a - 0.53B_b + \dots$ ${}^1\Psi ({}^1L_a) = 0.32L_b + 0.84L_a + 0.28B_a + 0.28B_b + \dots$ ${}^3\Psi ({}^3L_b) = 0.41L_b - 0.17L_a + 0.3B_a + 0.43B_b + \dots$ ${}^3\Psi ({}^3L_a) = 0.13L_b + 0.86L_a + 0.30B_a + 0.10B_b + \dots$
I-3-AA	${}^1\Psi ({}^1L_b) = 0.48L_b + 0.67L_a - 0.06B_a - 0.02B_b + \dots$ ${}^1\Psi ({}^1L_a) = -0.52L_b + 0.67L_a + 0.04B_a - 0.10B_b + \dots$ ${}^3\Psi ({}^3L_b) = 0.70L_b - 0.18L_a - 0.08B_a + 0.05B_b + \dots$ ${}^3\Psi ({}^3L_a) = 0.06L_b + 0.89L_a + 0.01B_a - 0.04B_b + \dots$
I-N-AA	${}^1\Psi ({}^1L_b) = 0.60L_b + 0.54L_a - 0.14B_a + 0.05B_b + \dots$ ${}^1\Psi ({}^1L_a) = -0.44L_b + 0.75L_a + 0.01B_a - 0.18B_b + \dots$ ${}^3\Psi ({}^3L_b) = 0.69L_b + 0.33L_a + 0.01B_a + 0.04B_b + \dots$ ${}^3\Psi ({}^3L_a) = -0.26L_b + 0.84L_a - 0.00B_a - 0.14B_b + \dots$
I-2-CA	${}^1\Psi ({}^1L_b) = 0.61L_b + 0.61L_a - 0.28B_a + 0.24B_b + \dots$ ${}^1\Psi ({}^1L_a) = 0.63L_b + 0.73L_a - 0.07B_a - 0.11B_b + \dots$ ${}^3\Psi ({}^3L_b) = 0.61L_b + 0.35L_a + 0.29B_a + 0.21B_b + \dots$ ${}^3\Psi ({}^3L_a) = 0.25L_b + 0.83L_a - 0.20B_a - 0.21B_b + \dots$
I-3-CA	${}^1\Psi ({}^1L_b) = 0.70L_b + 0.29L_a + 0.21B_a + 0.30B_b + \dots$ ${}^1\Psi ({}^1L_a) = -0.16L_b + 0.89L_a - 0.23B_a - 0.15B_b + \dots$ ${}^3\Psi ({}^3L_b) = 0.27L_b + 0.01L_a + 0.23B_a - 0.45B_b + \dots$ ${}^3\Psi ({}^3L_a) = -0.17L_b + 0.84L_a - 0.02B_a + 0.13B_b + \dots$
I-5-CA	${}^1\Psi ({}^1L_b) = 0.49L_b - 0.46L_a + 0.38B_a + 0.56B_b + \dots$ ${}^1\Psi ({}^1L_a) = 0.42L_b + 0.77L_a - 0.23B_a + 0.38B_b + \dots$ ${}^3\Psi ({}^3L_b) = 0.78L_b - 0.19L_a + 0.18B_a + 0.08B_b + \dots$ ${}^3\Psi ({}^3L_a) = 0.18L_b + 0.63L_a - 0.31B_a + 0.54B_b + \dots$
I-3-AL	${}^1\Psi ({}^1L_b) = 0.68L_b + 0.31L_a + 0.27B_a + 0.30B_b + \dots$ ${}^1\Psi ({}^1L_a) = -0.16L_b - 0.90L_a - 0.21B_a - 0.15B_b + \dots$ ${}^3\Psi ({}^3L_b) = 0.67L_b + 0.33L_a + 0.36B_a + 0.05B_b + \dots$ ${}^3\Psi ({}^3L_a) = -0.19L_b + 0.81L_a - 0.04B_a + 0.26B_b + \dots$

polarization spectrum with 280-m $\mu$  excitation, but the structure disappeared with 265-m $\mu$  excitation. Thus, they concluded that  ${}^3L_a$  lies mainly perpendicular to the molecular plane and to  ${}^1L_a$ , but it has a component along the  ${}^1L_b$  axis. We carried out the measurement of the polarized phosphorescence emission with 265-m $\mu$  excitation, as shown in Figure 11. It is apparent that the polarized phosphorescence spectra with 265-m $\mu$  excitation are structured and are more negatively polarized in some cases than the polarized phosphorescence spectra obtained with  ${}^1L_a$  excitation, particularly in the case of indole.

In the case of indole, this indicates that  ${}^1L_b$  contributes more to the singlet-triplet transition moment. This is in agreement with the previous work by Konev. However, the vibrational structure is qualitatively the same in both cases. In the other indoles (*e.g.*, indole-3-acetic acid, indole-3-carboxylic acid, and indole-3-aldehyde), the differential intensity contributions of  ${}^1L_a$  and  ${}^1L_b$  are not clearly demonstrated, as can be seen from Figure 11. Admittedly, further work with higher resolution instruments is needed. However, the polarized excitation spectra will aid in determining the differential contributions of  ${}^1L_a$  and  ${}^1L_b$  to the singlet-triplet transition moments, as will be discussed later. It should be pointed out that the  ${}^1L_a$  and  ${}^1L_b$  states interact strongly due to their close energy spacing. The interactions include vibronic couplings and configurational mixing between the two states both in the singlet and triplet manifold. At least the second type of interaction can be theoretically evaluated. This is shown in Table IV. It is readily apparent that the configurational interaction among L and B states is extensive. Nishimoto and Fujishiro<sup>63</sup> have theoretically examined the effect of configuration interaction of  ${}^1L_a$  and  ${}^1L_b$  states in naphthols. The theoretical results are

(63) K. Nishimoto and R. Fujishiro, *J. Chem. Phys.*, **36**, 3491 (1962).

that  $\alpha$ -naphthol possesses the same transition polarizations as in naphthalene, while  $\beta$ -naphthol is perturbed in this respect due to a strong configuration interaction between  ${}^1L_a$  and  ${}^1L_b$  states. In Table IV the contribution of the B states to the configuration interaction is also significant. In naphthalene, El-Sayed<sup>64</sup> showed strong vibronic interactions between the two low-lying singlet states. These interactions are probably reflected in the relative contribution of  ${}^1L_a$  and  ${}^1L_b$  states to the phosphorescence emission in indoles. Perkampus, *et al.*,<sup>65</sup> obtained the polarized phosphorescence spectra of phenanthroline derivatives with both  ${}^1L_a$  and  ${}^1L_b$  excitations. Their results are very similar to those shown in Figure 11.<sup>65</sup>

The polarized phosphorescence excitation spectra obtained using the emission wavelengths specified in Table I are shown in Figures 1-7, and they are all negatively polarized. Ideally, these polarization spectra should be obtained with the emission monitored at the 0-0 bands. In practice, this is almost impossible due to the weak 0-0 intensities in indoles. For this reason, the apparent phosphorescence maxima of the indoles were employed to obtain the polarized excitation spectra. Nonetheless, qualitative results are significant here. Namely, the excitation bands of  ${}^1L_a$  and  ${}^1L_b$  type are all negatively polarized, indicating again that the singlet-singlet transition moments are nearly perpendicularly oriented with respect to the singlet-triplet moments of the indoles studied. However, there appears to be a gradual increase in the degree of the excitation polarization in the long-wavelength region of

(64) M. A. El-Sayed, *ibid.*, **36**, 1943 (1962).(65) H.-H. Perkampus, A. Knop, and J. V. Knop, *Z. Naturforsch.*, **23a**, 840 (1968). The relative degree of the phosphorescence polarization of phenanthrolines are: 1,6 derivative, about the same with either  ${}^1L_a$  or  ${}^1L_b$  excitation; 2,6 derivative, slightly more negative with  ${}^1L_a$  than with  ${}^1L_b$ ; 3,6 derivative, considerably more negative with  ${}^1L_a$  than with  ${}^1L_b$ . In all three cases, vibrational structures are retained regardless of the excitation bands.

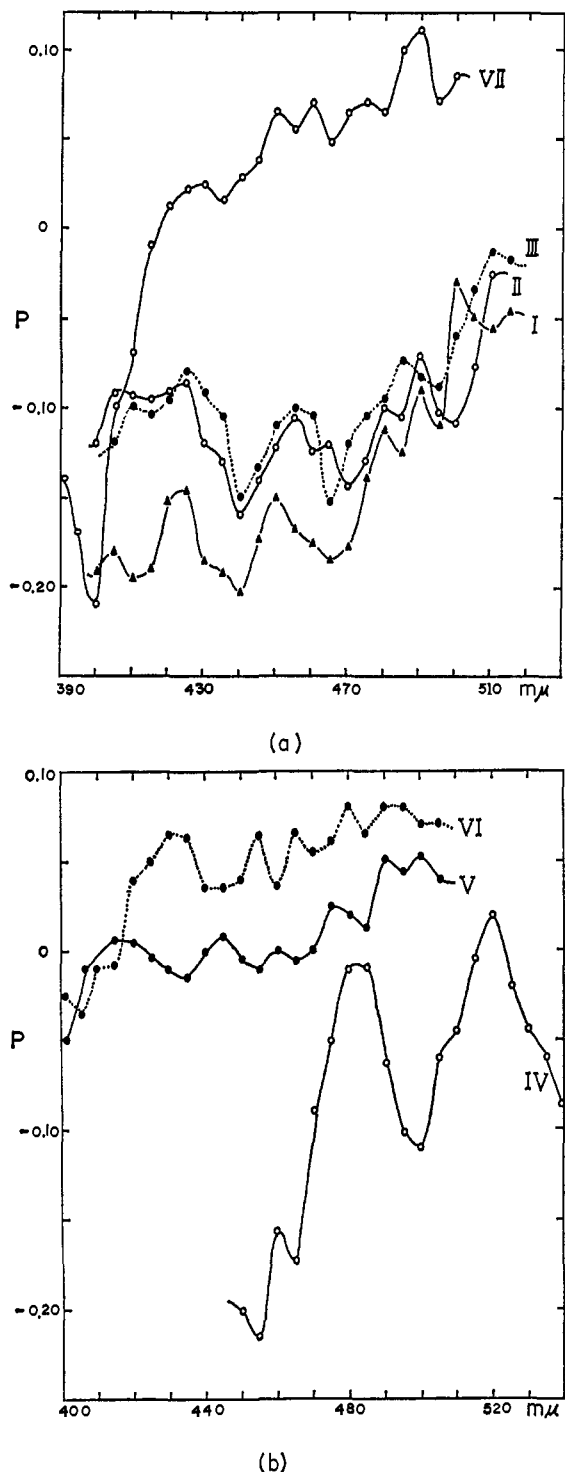


Figure 11. The polarized phosphorescence emission spectra of the indoles in EPA at 77°K, with excitation monitored at 265 m $\mu$ , which is rich in  $^1L_a$  components. (a) I, indole; II, indole-3-acetic acid; III, indole-N-acetic acid; and VII, indole-3-aldehyde. (b) IV, indole-2-carboxylic acid; V, indole-3-carboxylic acid; and VI, indole-5-carboxylic acid.

the excitation spectrum, indicating more effective vibronic spin-orbit and spin vibronic coupling between  $^1L_b$  and  $^3L_a$  than between  $^1L_a$  and  $^3L_a$ . The vibronic couplings may involve higher states ( $B$ 's,  $\sigma, \pi^*$ , and  $\pi, \sigma^*$ ) via non-totally symmetric modes. Notice that the phosphorescence excitation polarizations in most of the indoles studied increase again below 260 m $\mu$ . This is easily understood if one recalls that the ultraviolet peak cor-

responding to the minimum in the fluorescence excitation spectrum around 240 m $\mu$  is parallel to  $^1L_b$ .

Indole-5-carboxylic acid is unique in that the degree of the phosphorescence polarization becomes positive beyond the apparent 0-0 emission band, as can be seen in Figure 11. The 0-0 band region is also less negatively polarized in Figure 11 than in Figure 6. This uniqueness is further confirmed by the fact that the polarized phosphorescence excitation of this molecule shows a minimum degree of polarization in the  $^1L_b$ -rich region of the excitation spectrum, as shown in Figure 6. This clearly suggests that the vibronic spin-orbit and spin vibronic coupling are more important for the  $^1L_a$ - $^3L_a$  interaction than for the  $^1L_b$ - $^3L_a$  case. We do not know the definite reason for the peculiarity of this particular indole at present. However, the data shown in Table IV may be helpful in that the  $^3L_a$  state in indole-5-carboxylic acid more strongly interacts with  $^3B_a$  and  $^3B_b$  than any of the other indoles listed in Table IV. This is particularly true for the configuration interaction with  $^3B_b$ . In addition, the  $^1L_a$  state of indole-5-carboxylic acid is predicted to interact strongly with  $^1B_a$  and  $^1B_b$ . Vibronic interactions among these states undoubtedly contribute to the over-all spin-orbit coupling scheme in this molecule. The multicenter spin-orbit terms are also of importance in this regard. It should be pointed out here that indole-5-carboxylic acid is one of three indoles having a relative luminescence yield ratio higher than that of indole. Therefore, spin-orbit coupling schemes for indole-5-carboxylic acid must describe the contribution of the spin vibronic and vibronic spin-orbit coupling involving  $^1L_a$  and higher  $B$  states. The  $(n, \pi^*)$  state located in the carboxyl group may also be contributing, although the long lifetime does not reflect its significance (see footnote 67). The effect of the 3-carboxyl substituent in the case of indole-3-carboxylic acid is not clear. Apparently, the substitution enhances the spin-orbit coupling, as can be deduced from the higher luminescence ratio and the phosphorescence yield relative to indole.

Indole-3-aldehyde is most interesting because of its strong phosphorescence emission, shown in Figure 7 and Table II. Unlike the carboxyl indoles<sup>1,3</sup>  $(n, \pi^*)$ , states in indole-3-aldehyde are of lower energy. A consideration of the lowest virtual orbital energies and the oxygen atomic orbital coefficients of the molecular orbitals of the indoles as a measure of the  $^3(n, \pi^*)$  energy<sup>66</sup> qualitatively supports such a situation for indole-3-aldehyde. We attempted to locate the  $^1(n, \pi^*)$  in this molecule by looking at solvent shifts in the long-wavelength end of the absorption spectrum at different concentrations. No  $(n, \pi^*)$  state was located. The fact that the polarized phosphorescence spectrum (Figure 7) is nearly depolarized and the phosphorescence lifetime is significantly shorter than for the other indoles (Table II) is probably suggestive of the  $(n, \pi^*)$  role in the spin-orbit coupling mechanism. However, the lowest singlet state appears to be  $(\pi, \pi^*)$ . The CNDO calculations, without configuration interactions, indeed predict that the  $(n, \pi^*)$  is higher in energy (by 1.5 eV) than the lowest  $(\pi, \pi^*)$ .<sup>67</sup> Although fluorescence from

(66) C. Leibovici, F. Dupuy, and J. Deschamps, *Compt. Rend.*, **264B**, 299 (1967). Actual numerical calculations by this method are applicable only for quinone-like systems.

(67) The CNDO results correctly predict much higher energies (3-5 eV) for the  $(n, \pi^*)$  states in the 2- and 3-carboxyl derivatives than for

$^1(n,\pi^*)$  is known, the weak fluorescence in indole-3-aldehyde is most probably from a  $(\pi,\pi^*)$  rather than from an  $(n,\pi^*)$  state. Thus, the lack of appearance of an  $(n,\pi^*)$  absorption shoulder in nonpolar solvents and of occurrence of fluorescence suggests that the  $(n,\pi^*)$  may be hidden under the  $(\pi,\pi^*)$  bands.

The short lifetime (Table II) and very high phosphorescence to fluorescence ratio relative to indole (Table II), as well as the near-zero polarization of the polarized excitation spectrum and the positive polarization of the phosphorescence spectrum beyond the 0-0 emission band, are thus clearly indicative of the  $(n,\pi^*)$  contribution to the spin-orbit coupling scheme of this molecule. The role of the  $(n,\pi^*)$  in the singlet-triplet transition probability of indole-3-aldehyde probably lies in its vibronic coupling with  $(\pi,\pi^*)$  states either in the singlet or triplet manifold, followed by vibronic spin-orbit interactions. Vibronic interactions between  $(n,\pi^*)$  and  $(\pi,\pi^*)$  states, their contributions to the singlet-triplet intensity *via* vibronic spin-orbit coupling (second-order interactions), and their effects on polarizations and lifetimes have been demonstrated previously,<sup>41,53,68,69</sup> and were also invoked in the complex scheme of flavin molecules.<sup>10,70</sup> The positive polarization in the phosphorescence spectrum beyond the 0-0 emission band of indole-3-aldehyde (Figures 7 and 11a) can be explained by such a vibronic mechanism, since the interaction between  $(n,\pi^*)$  and  $(\pi,\pi^*)$  states introduces allowed  $\pi \rightarrow \pi^*$  transition moments (in-plane) into the singlet-triplet intensity. The  $^1(n,\pi^*)$  state (out-of-plane) can also spin-orbit couple directly with  $^3L_a$ , thus maintaining the negative degree of polarization of the 0-0 phosphorescence emission band (Figures 7 and 11a).

Whether the same mechanism can be invoked for the near-zero and positive phosphorescence polarizations of the indolecarboxylic acids (Figure 11b) is open for further studies. It will be particularly interesting to study what role the  $(n,\pi^*)$  in indole-5-carboxylic acid<sup>67</sup> plays in the polarization of its phosphorescence (Figures 6 and 11b), in view of the brief discussion given earlier.

Further work with high-resolution instruments is clearly needed in investigating the nature of the electronic perturbations introduced by carboxyl substituents. For example, this is necessary in order to elucidate (a) the effects of the substituent on the intensity of the vibronic bands of  $^1,^3L_a$ , which may strongly interact with upper states, and (b) the contribution of the vibronic interactions to the singlet-triplet transition probability and to the depolarization of the phosphorescence spectra. The role of  $(n,\pi^*)$  states originated from carboxyl substituents in the spin-orbit coupling is also an important question to be answered in order to fully interpret the polarized phosphorescence spectra of indolecarboxylic acids, as shown in Figure 11a. In order to do this, the energies of  $^1,^3(n,\pi^*)$  states localized on carboxyl sub-

indole-3-aldehyde. However, the predicted  $(n,\pi^*)$  in indole-5-carboxylic acid is located only 1.6 eV higher than the lowest  $(\pi,\pi^*)$ . Thus, the contribution of the  $(n,\pi^*)$  to the spin orbit coupling may be important. However, it should be emphasized that these energies are only qualitatively useful.

(68) (a) E. C. Lim and J. M. H. Yu, *J. Chem. Phys.*, **45**, 4742 (1966); (b) E. C. Lim and J. M. H. Yu, *ibid.*, **47**, 3270 (1967); (c) E. C. Lim and J. M. H. Yu, *ibid.*, **49**, 3878 (1968).

(69) H. Baba and T. Takemura, *Bull. Chem. Soc. Japan*, **40**, 2215 (1967).

(70) P. S. Song and W. E. Kurtin, *Photochem. Photobiol.*, in press.

stituents must be known in order to estimate the magnitude of the spin-orbit perturbation. In the meantime, we mention here that the magnitude is expected to be small, if the lifetimes of the indolecarboxylic acids shown in Table II are any indication of the  $(n,\pi^*)$  perturbations.

## Conclusions

We herein summarize our findings and conclusions therefrom. Dual emission from the  $^1L_a$  and  $^1L_b$  states of the indoles investigated has definitely been confirmed in both polar (glycerol-methanol) and relatively nonpolar (EPA) solvents. It has not been clearly established whether the dual emission occurs in indole-N-acetic acid. The  $^1L_b$  and  $^1L_a$  states in these indoles were partially resolved on the basis of fluorescence polarization spectra. The calculated energies are at least in qualitative agreement with the observed data. The polarization directions of the transition moments were also calculated, and are in excellent agreement with the observed polarizations, obtained from rather low-resolution measurements. It has been found that carboxyl, acetate, and formyl substituents do not reverse the Franck-Condon allowed  $^1L_a$  and  $^1L_b$  states, thus maintaining the spectroscopic correlation of indole with naphthalene. However, these substituents affect the electronic relaxation processes significantly. Indole-3-aldehyde, with a relatively low energy  $^1(n,\pi^*)$ , exhibited a weak fluorescence. Attempts to locate the  $(n,\pi^*)$  from the solvent effects on the absorption spectrum of indole-3-aldehyde were not successful. We therefore tentatively conclude that a  $(\pi,\pi^*)$  state is still the lowest singlet excited state in this molecule.

The 0-0 phosphorescence bands of these indoles were found to be negatively polarized, indicating possible spin-orbit coupling between  $(\sigma,\pi^*)$  or  $(\pi,\sigma^*)$  and  $^3L_a$  states. Considerable vibronic activities along the phosphorescence emission bands were revealed. In some cases (indole and indole-3-acetic acid), rough vibrational analyses were possible from our low-resolution polarization measurements. There appear to be two modes of vibrations: one with an approximate  $650\text{-cm}^{-1}$  series and another with a  $1500\text{-cm}^{-1}$  series. The former may be due to ring C-H or N-H out-of-plane bending and the latter could be a ring deformation (in-plane). It has been suggested that high-resolution measurements and vibrational analysis will aid in elucidating the role of carboxyl and formyl substituents in the singlet-triplet transitions of indoles. The apparent phosphorescence lifetimes of carboxyl derivatives were found to be relatively long. In addition, the carboxyl  $(n,\pi^*)$  states are probably too high in energy and low in oscillator strength to sufficiently contribute to direct spin-orbit couplings. However, indole-5-carboxylic acid is worthy of further study because of its high phosphorescence to fluorescence ratio. We have also found some contribution of the singlet-singlet ( $\pi \rightarrow \pi^*$ ) transition moments (in-plane) to the phosphorescence intensity *via* vibronic spin-orbit (second order) and spin vibronic (first order) interactions in most of the indoles studied. Two-center spin-orbit terms due to the nonplanar geometry of indole-N<sub>1</sub> provide interesting theoretical studies for the future.

The high phosphorescence to fluorescence ratio and the relatively short lifetime (0.6 sec) for indole-3-alde-

hyde are indicative of the significant role of  $^1,^3(n,\pi^*)$  states in this molecule. A large positive phosphorescence polarization beyond the 0-0 emission band has also been found in this molecule, suggesting vibronic involvement of  $(n,\pi^*)$  states in the spin-orbit interactions. However, whether vibronic coupling in the triplet manifold is more important than vibronic coupling in the singlet manifold has not been determined. It is felt that, for complicated molecules such as indole-3-aldehyde and other analogs, both vibronic coupling schemes are important in the over-all vibronic spin-orbit coupling. For example, Lamola has shown that both mechanisms are equally likely in acetophenone ( $^3L_a$ ).<sup>71</sup> It would be instructive to make a rough esti-

(71) A. A. Lamola, *J. Chem. Phys.*, **47**, 4810 (1967).

mate of the one-center spin-orbit contribution of the  $(n,\pi^*)$  localized on oxygen in indole-3-aldehyde. Using the procedure given by Plotnikov,<sup>72</sup> and adopting  $47.7\text{ cm}^{-1}$  for the spin-orbit coupling constant of atomic oxygen, the absolute square of the spin-orbit coupling matrix element was found to be  $303\text{ cm}^{-2}$ . The P-P-P wave function was used for this calculation. The calculated value is somewhat smaller in magnitude than was found for benzaldehyde ( $454\text{ cm}^{-2}$ ).<sup>72</sup> Like the other indoles studied in this work, the singlet-triplet split is large ( $7100\text{ cm}^{-1}$ ) for indole-3-aldehyde and is assigned as  $^3L_a$ . Lowest triplet states of the  $^3(n,\pi^*)$  type have been thoroughly investigated by Goodman and his coworker.<sup>73</sup>

(72) V. G. Plotnikov, *Opt. i Spectrosk.*, **20**, 735 (1966).

(73) R. Shimada and L. Goodman, *J. Chem. Phys.*, **43**, 2027 (1965).

## Chlorine-35 Nuclear Magnetic Resonance Study of Zinc Nucleotide Diphosphate Complexes<sup>1</sup>

J. A. Happe and R. L. Ward

Contribution from the Lawrence Radiation Laboratory, University of California, Livermore, California 94550. Received February 3, 1969

**Abstract:** In 0.5 M NaCl solutions, Zn(II)-nucleotide diphosphate complexes increase the  $^{35}\text{Cl}$  nuclear relaxation rate. The added relaxation is due to the formation of Zn(II)-Cl<sup>-</sup> bonds and has been studied by measuring the  $^{35}\text{Cl}$  nmr line width. The relaxation produced by unprotonated nucleotide diphosphate complexes is dependent on the nucleotide base structure. Maximum line broadening was found for the adenosine diphosphate complex, Zn-(ADP)<sup>-</sup>, while the inosine diphosphate complex, Zn(IDP)<sup>-</sup>, has the least effect. The relaxation produced by a given complex is influenced by protonation of the NDP ligand or by hydrolysis of the metal ion. The formation of Zn(ADP)<sub>2</sub><sup>4-</sup> is evident. The results strongly suggest that Zn<sup>2+</sup> is chelated between the nucleotide base and phosphate chain in Zn(ADP)<sup>-</sup> but is chelated only to the phosphate chain in Zn(IDP)<sup>-</sup>.

Both metal ions and enzymes are essential cofactors in the biochemical reactions of nucleotides.<sup>2</sup> It is also well known that there exists a high degree of enzyme specificity toward both the metal ion and nucleotide base structures. With this in mind, the structures of metal ion-ATP complexes have been studied extensively,<sup>3</sup> these being biochemically the most important nucleotides. A number of recent studies<sup>4-10</sup> have

sought to determine whether or not internal chelates were formed in which the metal ions were chelated both to the phosphate chain and to the nucleotide base moieties of ATP. All experimental evidence indicates that Mg<sup>2+</sup> and Ca<sup>2+</sup> bind only to the phosphate chain, whereas for other ions, such as Zn<sup>2+</sup>, Cu<sup>2+</sup>, and Mn<sup>2+</sup>, ring binding has often been indicated. There is no general agreement, however, on whether internal chelate formation takes place to a minor extent ( $\approx 15\%$ ) or whether it becomes essentially complete.<sup>10</sup> Little is known regarding the structures of the metal ion-nucleotide diphosphate complexes. The proton nmr results of Cohn and Hughes,<sup>4</sup> however, indicate that the Cu<sup>2+</sup> and Mn<sup>2+</sup> complexes of ADP may exist in the internally chelated form.

We wish to report a study of the Zn<sup>2+</sup> complexes of several nucleotide diphosphates by means of  $^{35}\text{Cl}$  nmr. Preliminary results on the ADP complexes have been reported earlier.<sup>11</sup> In these studies, Cl<sup>-</sup> ions have been used to monitor the Zn<sup>2+</sup> environment in these complexes as the nucleotide base structure is changed. Processes such as hydrolysis of the metal ion, the formation of complexes other than the 1:1 species, and protonation of the Zn(NDP)<sup>-</sup> complexes have been ex-

(1) This work was performed under the auspices of the U. S. Atomic Energy Commission.

(2) Nucleotide abbreviations used are: ATP for adenosine 5'-triphosphate; ADP, CDP, GDP, and IDP for adenosine, cytidine, guanosine, and inosine 5'-diphosphate; and NDP for a general nucleotide 5'-diphosphate. Where necessary, the charges and number of ionizable protons are indicated for a given molecule or ion, e.g., Zn-(ADPH)<sub>2</sub><sup>+</sup>, Zn(ADPH), Zn(ADP)<sup>-</sup>, ADPH<sub>2</sub><sup>+</sup>, etc. The formulas do not indicate proton positions.

(3) For a review of the literature prior to 1967, see R. Phillips, *Chem. Rev.*, **66**, 501 (1966).

(4) M. Cohn and T. R. Hughes, *J. Biol. Chem.*, **237**, 176 (1962).

(5) G. G. Hammes, G. E. Maciel, and J. S. Waugh, *J. Amer. Chem. Soc.*, **83**, 2394 (1961).

(6) G. G. Hammes and D. L. Miller, *J. Chem. Phys.*, **46**, 1533 (1967).

(7) J. A. Happe and M. Morales, *J. Amer. Chem. Soc.*, **88**, 2077 (1966).

(8) P. W. Schneider, H. Brintzinger, and H. Erlenmeyer, *Helv. Chim. Acta*, **47**, 1717 (1964).

(9) H. Sternlicht, D. E. Jones, and K. Kustin, *J. Amer. Chem. Soc.*, **90**, 7110 (1968).

(10) H. Sternlicht, R. G. Shulman, and E. W. Anderson, *J. Chem. Phys.*, **43**, 3133 (1965).

(11) R. L. Ward and J. A. Happe, *Biochem. Biophys. Res. Commun.*, **28**, 785 (1967).